Practical Analyses of Local Earthquakes

Nobuo HURUKAWA

International Institute of Seismology and Earthquake Engineering (IISEE)
Building Research Institute, Tsukuba, JAPAN

Preface

A single seismic station or local seismic network observes local earthquakes. What can we do using seismic wave records? We can determine their hypocenters, magnitudes, focal mechanisms, crust and upper mantle structure etc. In this lecture note, you will learn how to pick up *P*- and *S*-wave arrival times correctly as well as other later phases and how to measure amplitudes from observed seismic wave records. These phase data and seismographs will be analyzed by different methods to know hypocenters and magnitudes of earthquakes. I hope you will understand basic characteristics of local earthquakes by analyzing seismograms practically.

The Original version of this lecture note was published in 1995 by Japan International Cooperation Agency (JICA).

December 2008

Nobuo HURUKAWA, IISEE

(Slightly revised on 2012/12/17)

CONTENTS

1. Introduction 1

1.1 Classification of Earthquakes 1

1.2 Seismic Waves of Local Earthquakes 1

2. Wadati Diagram 3

2.1 Procedure 4

2.2 Origin Time 6

2.3 Hypocentral Distance 7

2.4 *Vp*/*Vs* Ratio 8

2.5 Examination of Reading Data 9

3. Particle Motion 18

3.1 Procedure 18

3.2 Incident Angle 20

3.3 Phase Identification 21

4. Apparent Velocity 26

4.1 Procedure 26

4.2 Tripartite 27

4.3 Seismic Array 29

4.4 Application of Apparent Velocity 30

5. Hypocenter Determination 32

5.1 Graphical Method 32

5.2 Calculative Method 36

5.3 Travel-Time Table 45

5.4 Conversion of (λ, φ) to (x, y) 46

5.5 HYPO71PC 48

6. Magnitude 51

6.1 Velocity Amplitude Magnitude 51

6.2 *F*-*P* Magnitude 51

6.3 Magnitude Scales Used by ISC and NEIS 54

Chapter 1 Introduction

Local seismic networks range from several tens to several hundreds of kilometers, with stations spaced 10 to several tens of kilometers apart. Since such a network uses high-sensitivity short-period velocity seismographs, mainly microearthquakes are observed. The main objective of these lecture notes is to explain how to locate earthquakes. Although their arrival times at stations are mainly used, methods are also given that use waveforms, as are simple methods to obtain the hypocenter and the magnitudes of earthquakes.

1.1 Classification of Earthquakes

Earthquakes are classified with respect to their magnitudes as follows:

$M \geqq 7$: Large earthquakes

$M < 7$: Middle earthquakes

$M < 5$: Small earthquakes

$M < 3$: Microearthquakes

$M < 1$: Ultra microearthquakes

The largest instrumental earthquake is the 1960 Chilean earthquake, M =9.5. The size of the earthquake fault involved is 800 x 200 km^2 with a dislocation of 30 m and the seismic moment 2.7 x 10^{30} dyn·cm (Kanamori and Cipar, 1974). In contract, one of the smallest known is an M =-2.7 earthquake for which the *S*-*P* time is 55 ms (Iio, 1986).

1.2 Seismic Waves of Local Earthquakes

Examples of the crustal waves of local and regional earthquakes are shown in Kulhanek (1990). Recording distances of these waves are 0-10°. The following three types of phases are observed:

Pg and *Sg* are direct *P* and *S* waves.	*Vp* = 5.8-6.2 km/s
*P** and *S** are *P* and *S* waves refracted at the Conrad discontinuity.	*Vp* = 6.5-7.2 km/s
Pn and *Sn* are *P* and *S* waves refracted at the Moho discontinuity.	*Vp* = 7.5-8.2 km/s

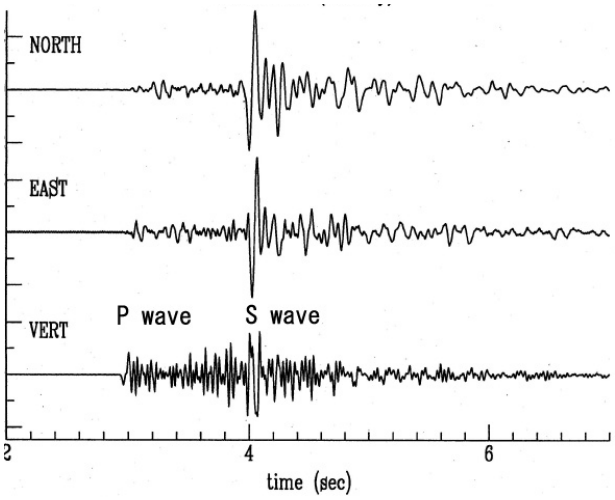

Fig. 1.1 Three-component seismogram of a local earthquake recorded by a velocity-type seismograph.

Exercise 1.1 Measure maximum amplitude and its frequency of a *P* wave on a vertical-component seismogram at a station shown in Fig. 1.1. Then, obtain the maximum velocity amplitude. Suppose the following constants for seismograms:

Sensitivity of seismometer: 4.0 V/kine

Amplification of amplifier: 1.0^3 (1,000) times

Amplification on paper: 2.5 mm/V

Note: kine is a unit of velocity. kine = cm/s

Exercise 1.2 Convert the maximum velocity amplitude obtained above to displacement and acceleration assuming the following sinusoidal wave:

$$x = a\sin(2\pi ft)$$

x : displacement
a : amplitude
f : frequency
t : time

References

Iio, Y., 1986, Ultramicroearthquakes (M=-3) which occurred near the ground surface -Aftershocks of the western Nagano prefecture earthquake of Sep. 14, 1984-, Zisin (J. Seismol. Soc. Japan), 39, 645-652 (in Japanese with English abstract).

Kanamori, H. and Cipar, J. J., 1974, Focal process of the Chilean earthquake May 22, 1960, Phys. Earth Planet. Inter., 9, 128-136.

Kulhanek, O., 1990, Anatomy of Seismograms, Developments in Solid Earth Geophysics, Ser. 18, Elsevier

Chapter 2 Wadati Diagram

The most primitive analysis of local earthquakes uses a *Wadati diagram*. We use only *P*- and *S*-wave arrival times in this analysis. An *S*-*P* time is a time difference between *P*- and *S*- wave arrival times, and is very often used in analyses of local earthquakes. The *Wadati diagram* is used for the following four purposes:

1. To obtain the origin time of an earthquake.
2. To calculate the hypocentral distance.
3. To obtain the *Vp/Vs* ratio (or Poisson's ratio) in medium.
4. To examine *P* and *S* readings.

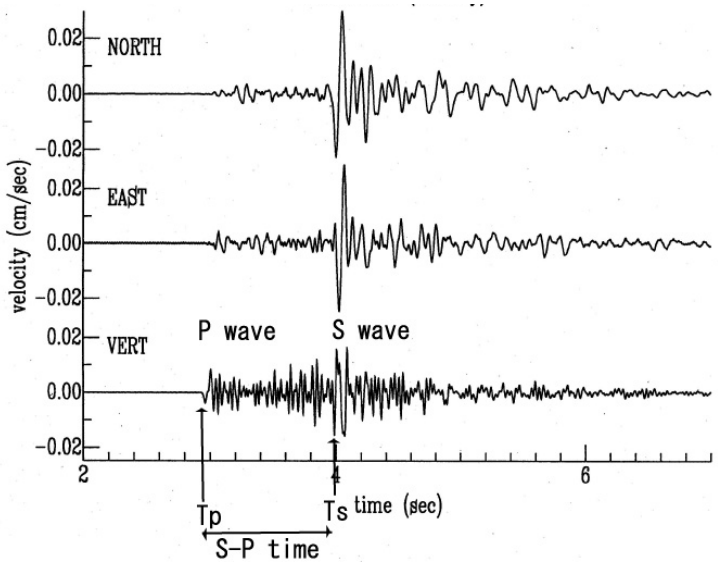

Fig. 2.1 Three-components waveforms of a local earthquake.

2.1 Procedure

The *Wadati diagram* is as follows if we observe one earthquake at several stations:

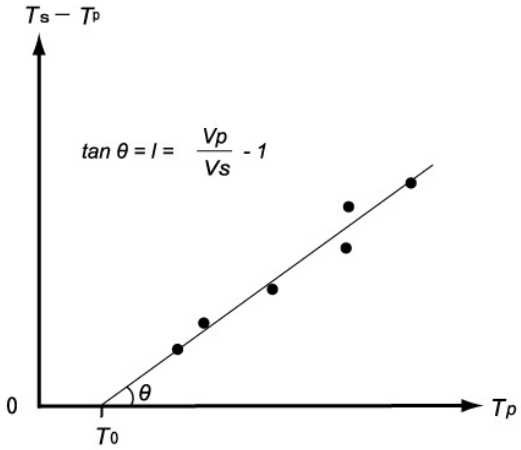

Fig. 2.2 Wadati diagram.

First, plot an *S*-*P* time against a *P*-wave arrival time at each station. Second, fit a straight line to all data. There are two ways to fit the straight line:

Method 1: When we have little data of poor quality, we fit a straight line with a given slope *l*, where $l = Vp/Vs - 1$. This implies that we assume a *Vp*/*Vs* ratio.

Method 2: When we have much data of good quality, we may fit a straight line freely, and can obtain the slope of the line.

The origin time of the earthquake is obtained from the intercept of the *P*-time axis when an *S*-*P* time is zero in either way.

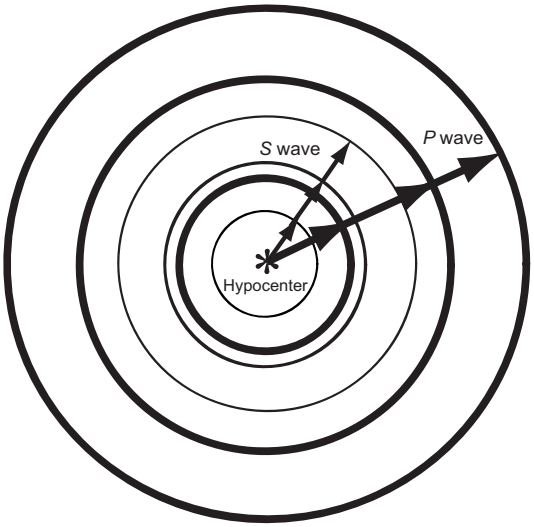

Fig. 2.3 Emanation and propagation of *P* and *S* waves from the hypocenter. The *P*-wave speed is about 1.7 times faster than the *S*-wave speed.

Why is all data on the straight line? This is because two waves with different velocities emanate from the same point simultaneously as shown in Fig. 2.3. We can therefore tell the distance between the source and observation point using the travel time difference between the two waves.

The principle of the *Wadati diagram* is as follows, assuming that the medium is homogeneous and using following notations:

Tp: *P*-wave arrival time
Ts: *S*-wave arrival time
To: Origin time
Tpo: *P*-wave travel time (=*Tp*-*To*)
Tso: *S*-wave travel time (=*Ts*-*To*)
Tsp: *S*-*P* time (=*Ts*-*Tp*)
Vp: *P*-wave velocity
Vs: *S*-wave velocity
D : Hypocentral distance

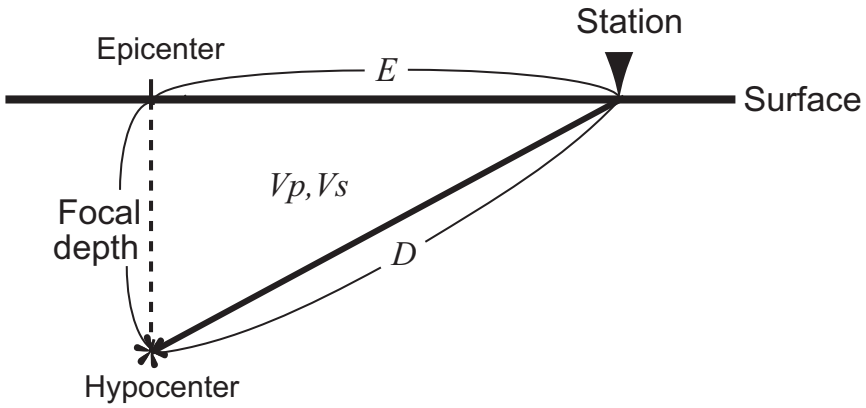

Fig. 2.4 Hypocentral distance *D*, epicentral distance *E*, and focal depth.

A hypocentral distance is represented by *P*-and *S*-wave travel times and velocities as follows:

$$D = Tpo * Vp \tag{2.1}$$

$$D = Tso * Vs = (Ts - To) * Vs = \{(Ts - Tp) + (Tp - To)\} * Vs = (Tsp + Tpo) * Vs \tag{2.2}$$

From equations (2.1) and (2.2)

$$Tpo * Vp = (Tsp + Tpo) * Vs,$$

then

$$Tpo * (Vp - Vs) = Tsp * Vs. \tag{2.3}$$

Therefore

$$Tsp = \left(\frac{Vp}{Vs} - 1 \right) * Tpo$$

and

$$Tsp = \left(\frac{Vp}{Vs} - 1 \right) * (Tp - To). \tag{2.4}$$

Then,

$$Tsp = l * Tpo.$$

This is also valid in a layered media with a constant *Vp*/*Vs* ratio. Since

$$Tpo = \int \frac{ds}{Vp}, \quad Tso = \int \frac{ds}{Vs},$$

then

$$Tsp = Tso - Tpo = \int \left(\frac{1}{Vs} - \frac{1}{Vp} \right) ds = \int \left(\frac{Vp}{Vs} - 1 \right) \frac{ds}{Vp} = \left(\frac{Vp}{Vs} - 1 \right) Tpo = lTpo,$$

where

$$l = \frac{Vp}{Vs} - 1. \tag{2.5}$$

Exercise 2.1 We use data from the National Research Institute for Earth Science and Disaster Prevention (NIED, Fig. 2.5) in this exercise.

(1) Read onsets of *P* and *S* waves of the event shown in Fig. 2.6.

(2) Make a *Wadati diagram* for this event and obtain the origin time and *Vp/Vs* ratio.

2.2 Origin Time

From equations (2.4) and (2.5), the origin time of the earthquake is represented by *Tp*, Tsp and *l* as follows:

$$To = Tp - \frac{Tsp}{l}. \tag{2.6}$$

This relation is also clearly shown in Fig. 2.2.

When the number of data points is greater than one, we calculate the origin time by a least-squares method. We obtain *To* and *l* that minimize

$$\sum_{i=1}^{n} \left[To - \left(Tp_i - \frac{Tsp_i}{l} \right) \right]^2,$$

where Tp_i, Tsp_i and *n* are *P* and *S*-*P* times at the *i*-th station and a number of stations, respectively. When we assume *l*, *To* is obtained easily as follows:

$$To = \frac{1}{n} \sum_{i=1}^{n} \left(Tp_i - \frac{Tsp_i}{l} \right).$$

This implies that the origin time is an average of origin times calculated at all stations individually.

This is the easiest method for obtaining the origin time of an earthquake.

Exercise 2.2 Let's use the same event as Exercise 2.1.

(1) Obtain the origin time of the event by equation (2.6) using data at station ASG. Assume that $Vp/Vs = 1.73$.

(2) Using the *Wadati diagram* obtained in Exercise 2.1, obtain the origin time by method 1 assuming $Vp/Vs = 1.73$.

2.3 Hypocentral Distance

From equations (2.1) and (2.3), the hypocentral distance is represented as follows:

$$D = Tpo * Vp = \frac{Tsp * Vs}{Vp - Vs} Vp$$

Therefore

$$D = \frac{Vp}{\frac{Vp}{Vs} - 1} Tsp. \qquad (2.7)$$

We can represent a hypocentral distance by *S-P* time, *Vp* and *Vp/Vs* ratio. If we regard *Vp* and *Vp/Vs* as constant, we can calculate *D* very easily by measuring only *S-P* time. Put

$$k = \frac{Vp}{\frac{Vp}{Vs} - 1}, \qquad (2.8)$$

Then

$$D = k * Tsp. \qquad (2.9)$$

We call *k* the *Oomori coefficient*. Since *Vp* is 5.7-6.0 km/s and *Vp/Vs* is about 1.73 in the upper crust of the Earth, where almost all earthquakes occur, *k* is about 8 km/s. A hypocentral distance is easily calculated by an *S-P* time multiplied by 8. Note that *Vp* is about 4 km/s and *Vp/Vs* is about 1.8 in volcanic regions. Then *k* is about 5.

If a hypocentral distance is several times larger than a focal depth for shallower earthquakes, an epicentral distance is nearly equal to the hypocentral distance. We can therefore estimate the epicentral distance, which is more commonly used in seismology than the hypocentral distance, in a *Wadati diagra*m.

This method for calculating a hypocentral distance is the same as the method for determining the place where lightning strikes using the time difference (*Tdif*) between the lightning flash and the sound of thunder. Suppose *Vso* and *Vli* are velocities of sound (340 m/s) and light (3 x 10^8 m/s), respectively. We put *Vli* and *Vso* instead of *Vp* and *Vs*, respectively in equation (2.7) as

follows:

$$D = \frac{Vli}{\frac{Vli}{Vso} - 1} * \mathrm{Tdif} = \frac{Vso}{1 - \frac{Vso}{Vli}} * Tdif$$

Since *Vli* is much greater than *Vso*, we get the following formula:

$$D = Vso * Tdif = 340 Tdif \,(\mathrm{m}).$$

Exercise 2.3

(1) Calculate *Oomori coefficient k* when *Vp* and *Vp/Vs* are 6.0 km/s and 1.73, respectively

(2) Calculate a hypocentral distance at *Tsp* = 10 s assuming *k* obtained in (1).

2.4 *Vp/Vs* Ratio

As stated in the elasticity theory in the lecture on "Theory of Seismic Waves" (Geller, 1993), *P*- and *S*-wave velocities are represented as follows from an equation of motion for an isotropic elastic body:

$$Vp = \sqrt{\frac{\lambda + 2\mu}{\rho}}, \quad Vs = \sqrt{\frac{\mu}{\rho}}$$

$$\frac{Vp}{Vs} = \sqrt{\frac{\lambda}{\mu} + 2} = \sqrt{\frac{2(1-\sigma)}{1-2\sigma}}.$$

Table 2.1

σ	0.20	0.25	0.30
$\frac{Vp}{Vs}$	1.63	1.73	1.87

(From *Hook's law* on an isotropic elastic body)

where λ, μ: *Lame*'s constants

μ: Rigidity

σ: *Poisson*'s ratio

ρ: Density

when $\lambda = \mu$, σ = 0.25, *Vp/Vs* = 1.73, and *Tsp* = 0.73*Tpo*. Since μ = 0 (σ = 0.5) in liquid, a liquid does not transmit *S* waves.

It is easier to obtain *Vp/Vs* ratios than *P*- and *S*-wave velocities, because we must know the

hypocenters of earthquakes used in analyses to obtain *P*- and/or *S*-wave velocities. If we use the *Wadati diagram*, we can obtain *Vp/Vs* ratios without earthquake locations used. Therefore, this method is widely used in analyses of crust and upper mantle structures (e.g., Ukawa, 1981) and studies of temporal changes in seismic velocities (e.g., Aggarwal et al., 1973; Semenov, 1969).

Exercise 2.4 Using the *Wadati diagram* obtained in Exercise 2.1, obtain the origin time, a *Vp/Vs* ratio and a *Poisson*'s ratio by method 2.

2.5 Examination of Reading Data

We usually judge the quality of reading data by travel-time residuals. When we locate hypocenters, we calculate travel-time residuals and omit reading data with large residuals. However, if we use a *Wadati diagram*, we can check the quality of reading data before locating earthquakes. Since there is a linear relation between *Tsp* and *Tp* as shown in Fig. 2.2 and in equation (2.4), all the reading data should satisfy this relation. Data that are not on the straight line in the *Wadati diagram* is unreliable. We should carefully reexamine such data.

References

Aggarwal, Y. P.,Sykes, L. R.,Armbruster, J., and Sbar, M. L., 1973, Premonitory changes in seismic velocities and prediction of earthquakes, Nature, 241, 101-104.

Geller, R. J., 1993, The theory of elasticity and its application to seismology, IISEE Lecture Notes.

Semenov, A. M., 1969, Variations in the travel-time of transverse and longitudinal waves before violent earthquakes, Izv. Acad. Sci. USSR, Earth Phys., No. 4, 72-77.

Ukawa, M. and Fukao, Y., 1981, Poisson's ratios of the upper and lower crust and the sub-Moho mantle beneath central Honshu, Japan, Tectonophysics, 77, 233-256.

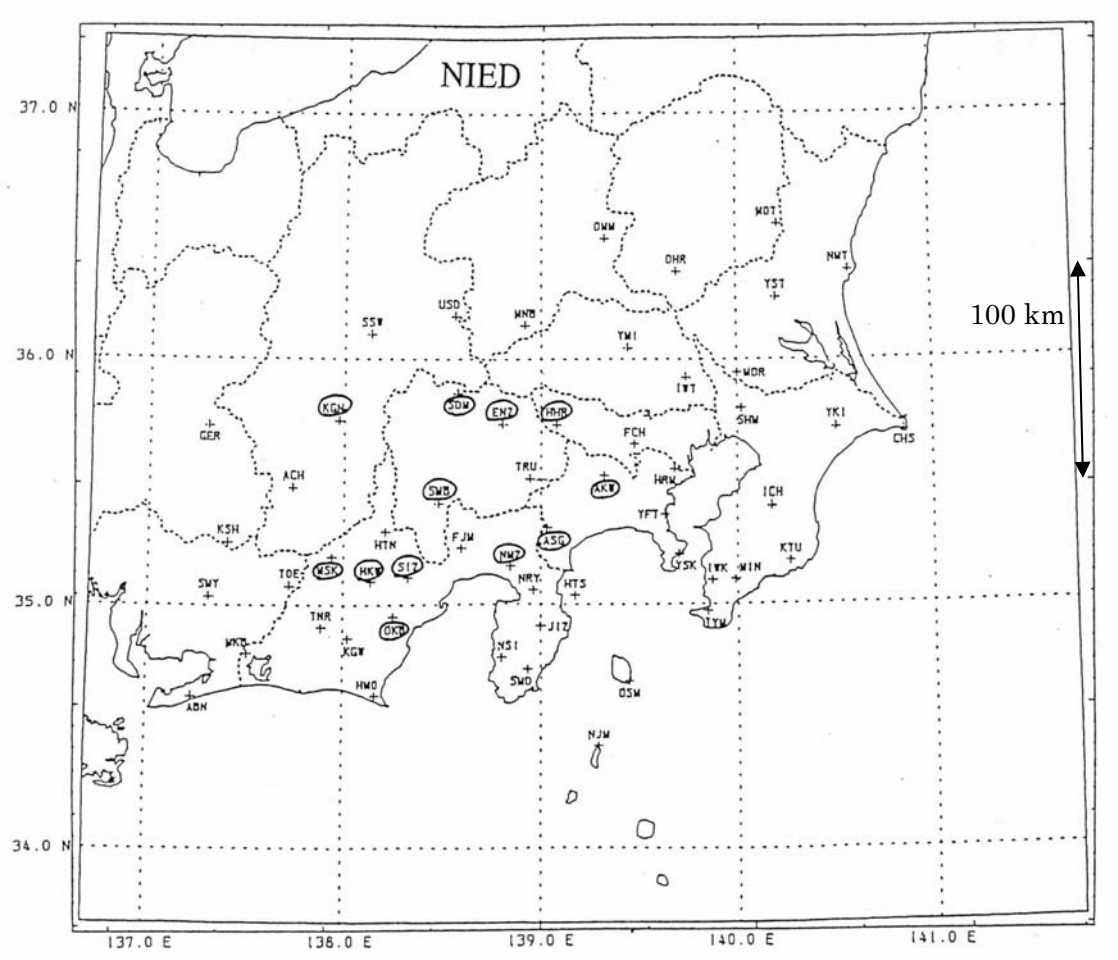

Fig. 2.5 Location of observation stations of the National Research Center for Earth Science and Disaster Prevention (NIED) as of 1983. Encircled stations are used in these lecture notes.

Table 2.2 Coordinates and (X, Y) coordinates of NIED stations.
The origin of (X, Y) coordinate is (35.5°N, 139°E).

	Code	Lat. (°N)	Lon. (°E)	Z, m	X, km	Y, km
1	ASG	35.3167	139.0247	386	2.537	-20.658
2	HHR	35.7385	139.0732	605	6.912	26.110
3	ENZ	35.7392	138.8019	801	-17.613	26.202
4	AKW	35.5232	139.3149	-8	28.836	2.276
5	NMZ	35.1609	138.8431	109	-14.013	-37.977
6	SMB	35.4189	138.4803	201	-46.920	-9.231
7	SDM	35.8675	138.5739	1,270	-38.205	40.502
8	SIZ	35.1147	138.3267	77	-61.116	-42.885
9	HKW	35.0966	138.1351	339	-78.600	-44.792
10	OKB	34.9532	138.2506	-31	-68.160	-60.764
11	KGN	35.7550	137.9688	630	-92.986	28.421
12	MSK	35.1983	137.9358	720	-96.617	-33.500

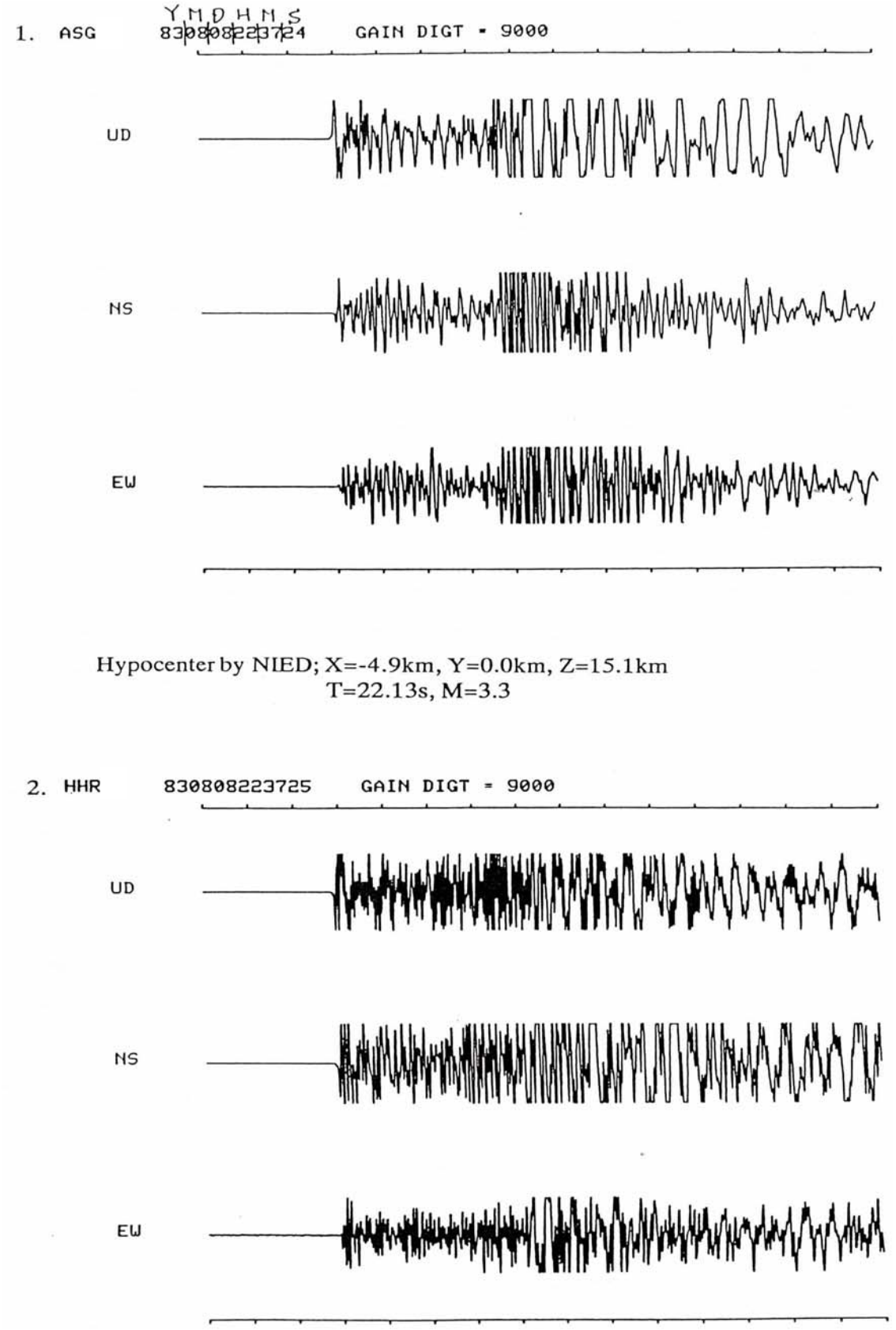

Fig. 2.6 Three-component seismograms at 12 stations of NIED. The interval of the time mark is one second. The starting time of records at each station is shown on the right of a station code.

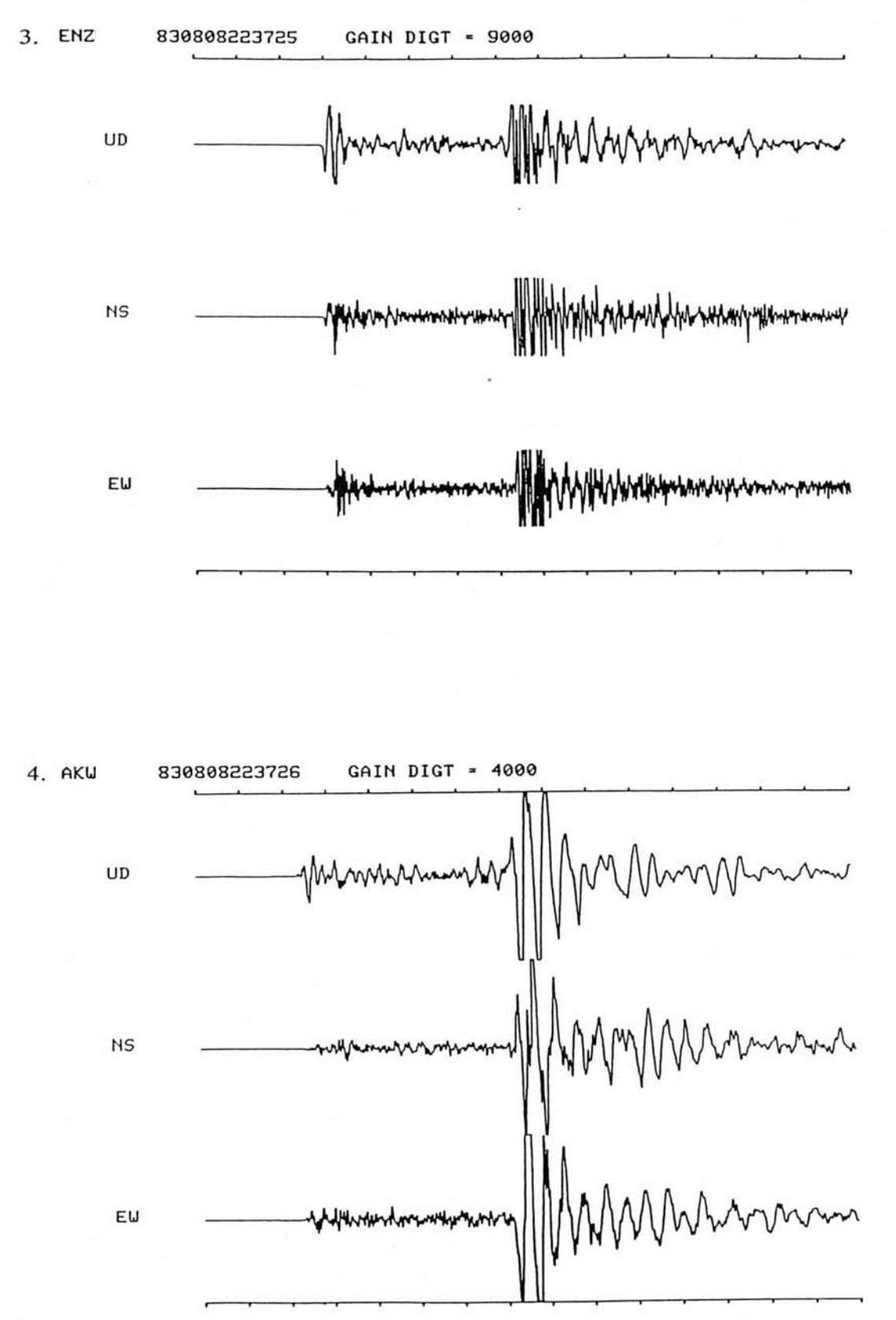

Fig. 2.6 (continued)

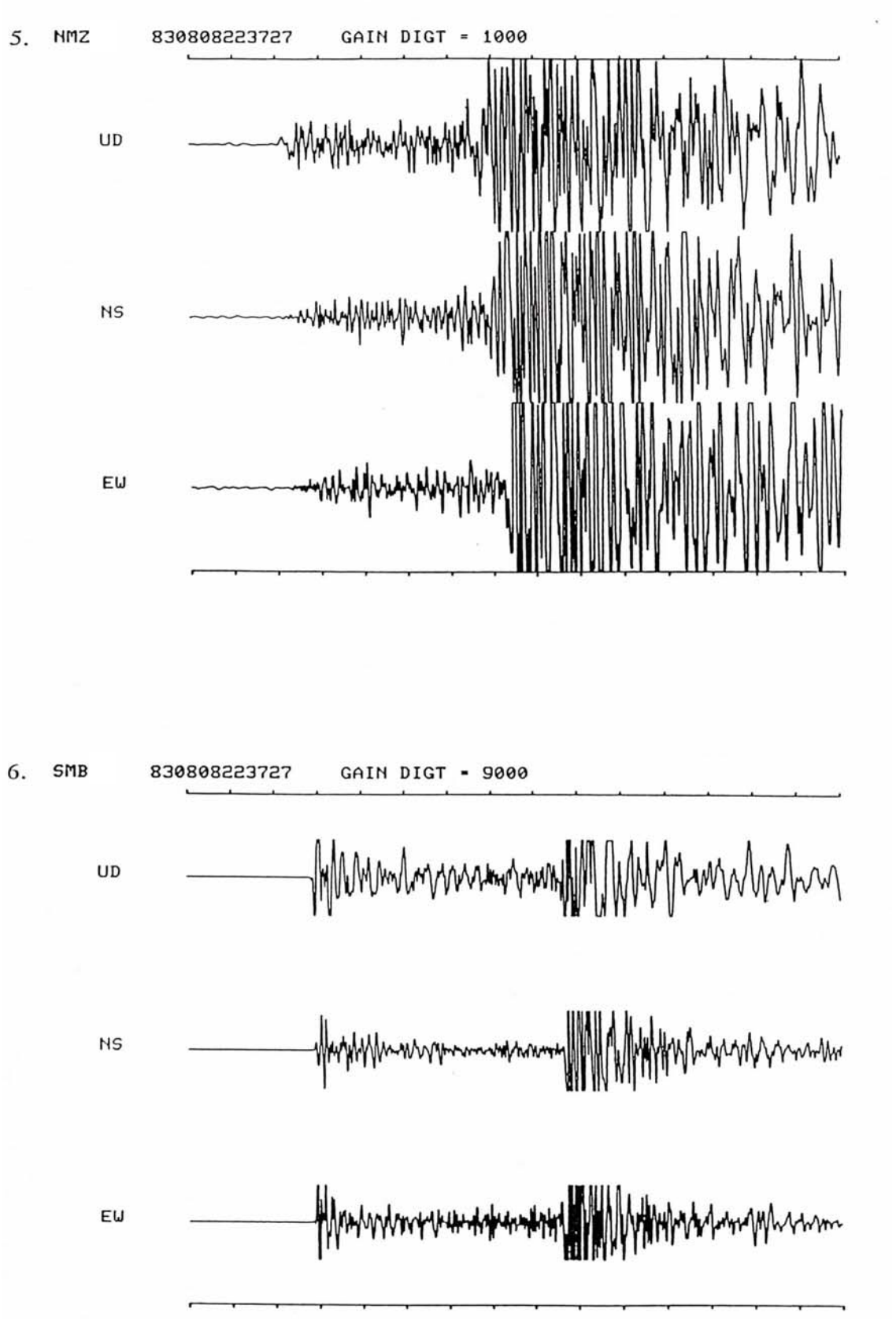

Fig. 2.6 (continued)

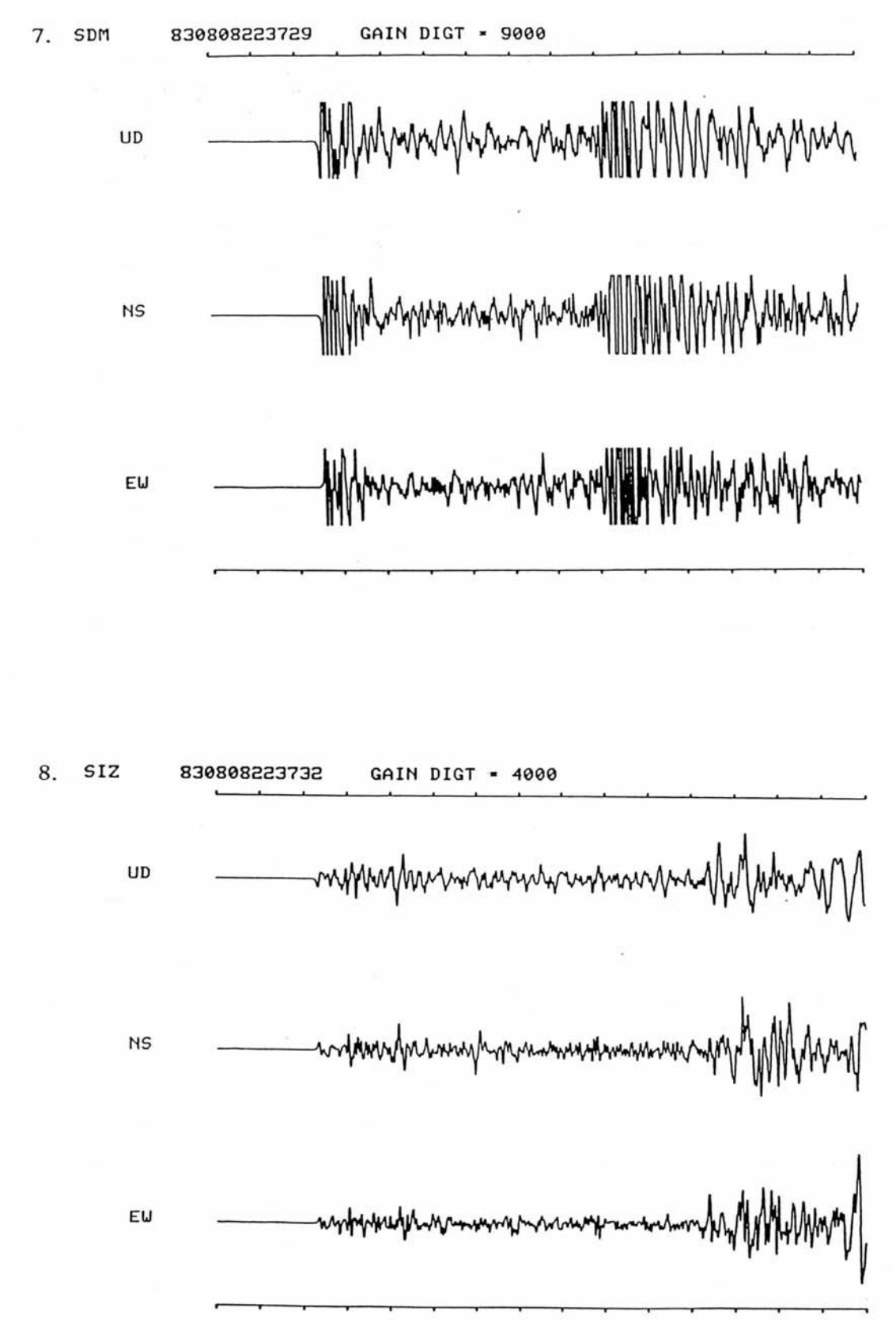

Fig. 2.6 (continued)

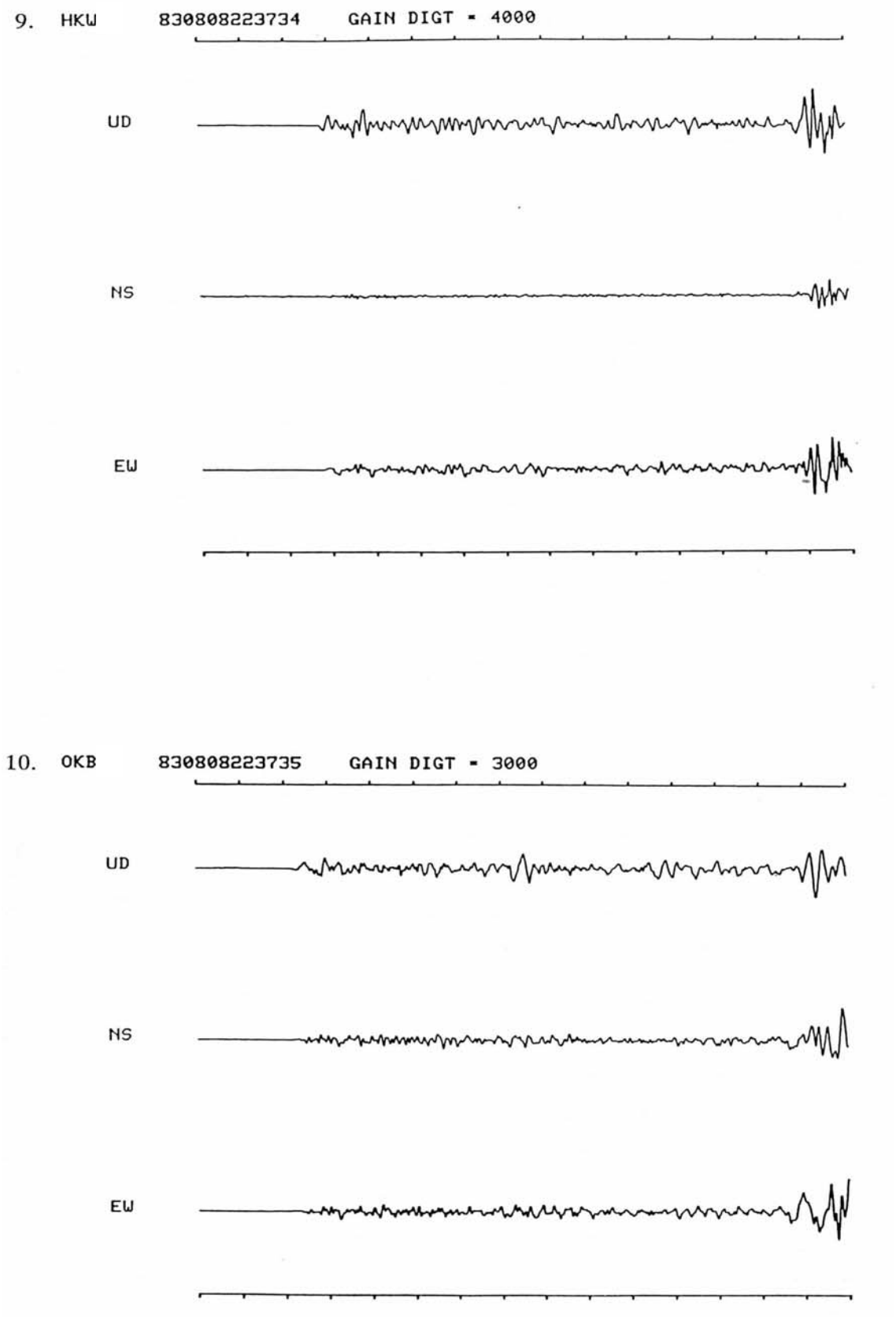

Fig. 2.6 (continued)

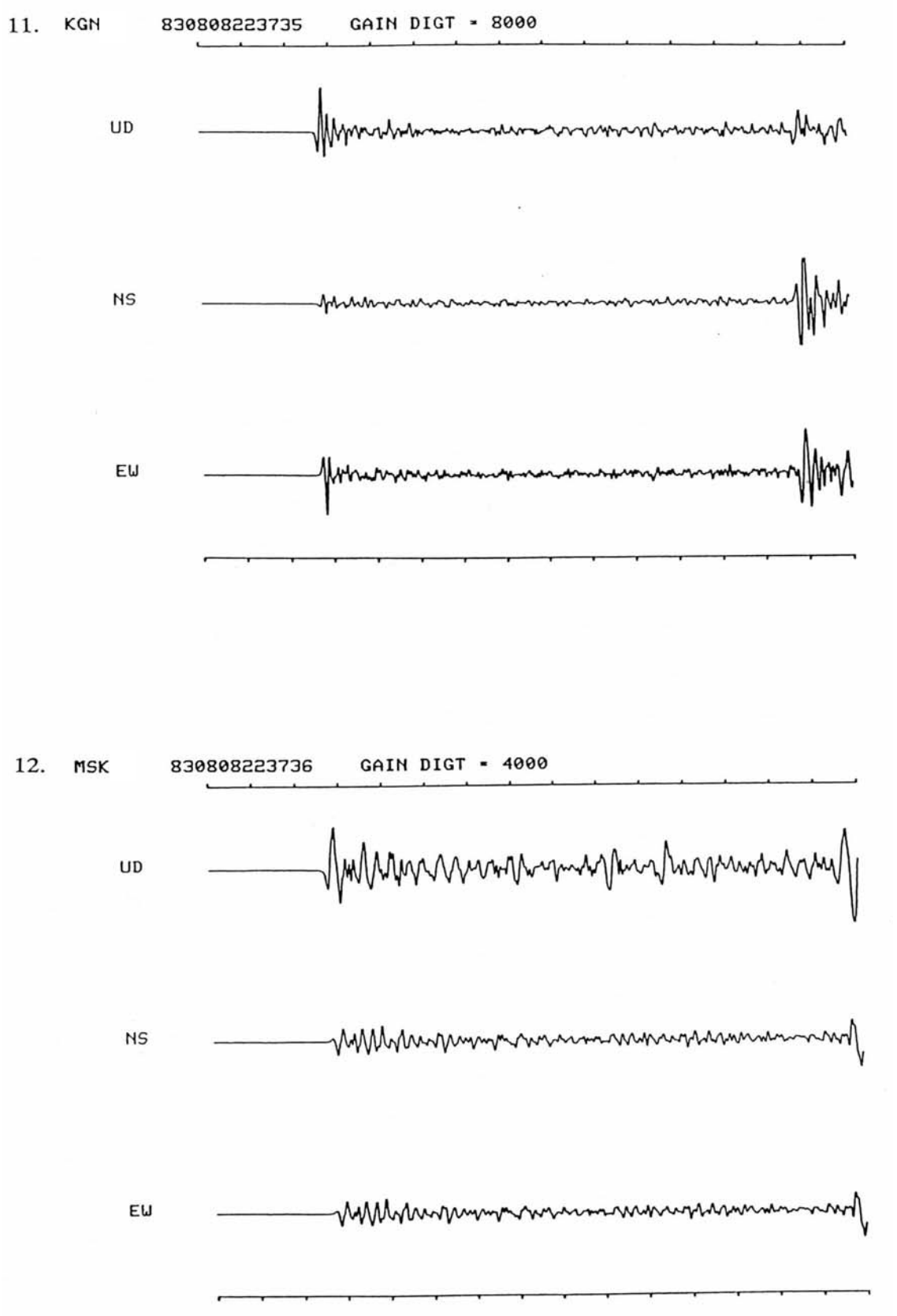

Fig. 2.6 (continued)

Chapter 3 Particle Motion

In this chapter, we analyze waveforms recorded on three-component seismograms at one station. Since we use amplitudes of seismic waves, an amplification of each component should be known to determine a particle motion correctly. The particle motion, or locus, is the motion of ground where the seismograph is. Purposes for using it are as follows:

1. To know the direction of wave approach or the direction to an epicenter.
2. To know the incident angle to the surface and the apparent velocity of an observed wave.
3. To know the type of an observed wave.

In addition, we will learn a method to locate earthquakes observed only at one station.

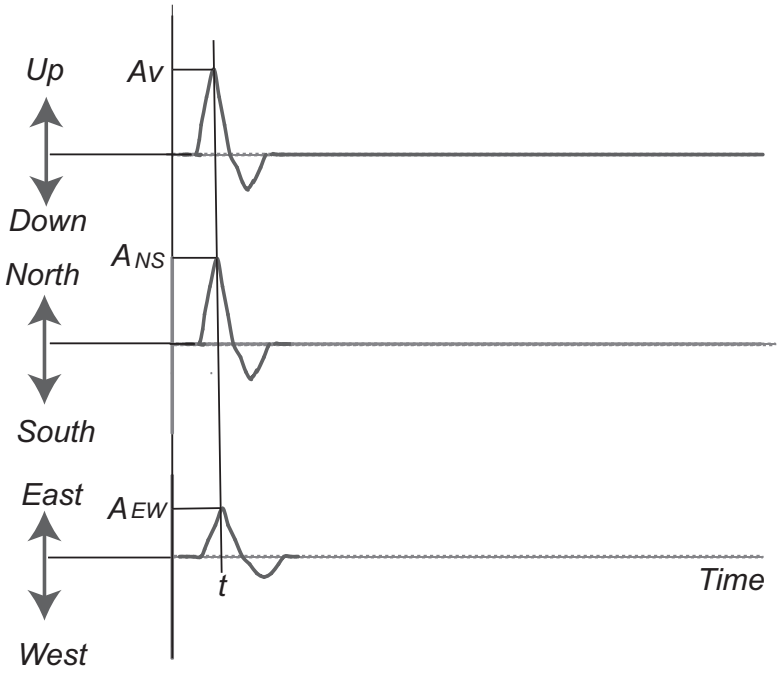

Fig. 3.1 Initial *P* waves in three-component seismograms.

3.1 Procedure

To obtain the particle motion of an observed seismic wave, suppose amplitudes of vertical and two horizontal (North-South and East-West) component seismograms are A_V, A_{NS}, and A_{EW}, respectively, at a certain time.

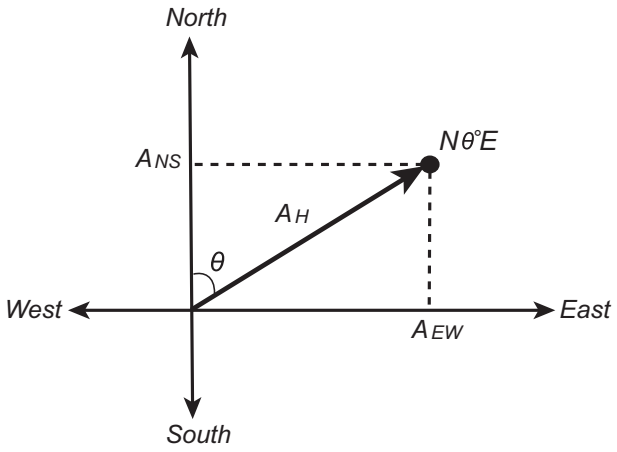

Fig.3.2 Horizontal plane view.

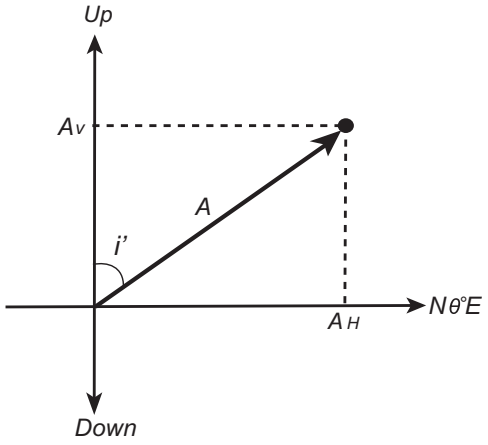

Fig. 3.3 View on vertical plane parallel to the ray path.

3.1.1 Horizontal motion

First, we obtain the total horizontal amplitude and a direction of a vibration using two horizontal-component seismograms. Plot A_{NS} against A_{EW}. The total horizontal amplitude at this time and the direction of the particle motion are as follows: (In case that both A_{NS} and A_{EW} are positive.)

$$A_H = \sqrt{A_{NS}{}^2 + A_{EW}{}^2}$$

$$\theta = \tan^{-1}\frac{A_{EW}}{A_{NS}}.$$

When we analyze the initial *P* wave, the direction to the epicenter of the earthquake is parallel to the direction of the *P*-wave particle motion, that is N θ^{o}E.

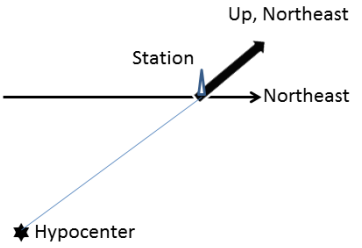

Fig. 3.3-2. Particle motion and the hypocenter.

3.1.2 Vertical motion

Second, we obtain the total amplitude and the apparent incident angle. Plot A_V against A_H. Angle i' in Fig. 3.3 is called the apparent incident angle, which is not the same as the true incident angle. Total amplitude A and apparent incident angle i' are represented by A_V and A_H as follows:

$$A = \sqrt{A_V{}^2 + A_H{}^2}$$

$$i' = \tan^{-1}\frac{A_H}{A_V}$$

When we analyze the initial *P* wave, the direction to the epicenter of the earthquake is easily obtained as follows: Since this direction is parallel to the direction of the *P*-wave particle motion, the direction is Nθ^{o}E when the polarity of the *P* wave is down. Otherwise, it is N(θ+180°)E. The reason is that the *P* wave travels in underground, not through air.

Since we can estimate a hypocentral distance from the *S*-*P* time as learned in Chapter 2, we can roughly estimate the epicenter of the earthquake:

Cf., $D = \frac{Vp}{l} Tsp$ where $l = \frac{Vp}{Vs} - 1$

3.2 Incident Angle

The incident angle of the seismic wave is the angle between the ray path and the vertical line. It is used for the following purposes:

1. To obtain a velocity in a surface layer at a station when an apparent velocity of the seismic wave is known.
2. To obtain an apparent velocity of the seismic wave observed at a station when a velocity in the surface layer is known.

The angle between the direction of a particle motion at the surface and the vertical axis is called an apparent incident angle, which is not the same as a true incident angle. We can obtain the apparent incident angle by a three-component seismic observation as shown in Section 3.1, but we cannot obtain the true incident angle without knowledge of the underground velocity structure. Put

i: *P* incident angle

j: *S* incident angle

i': Apparent incident angle

Vap: Apparent velocity

We get the following relation:

$$i' = 2j$$

This equation is derived from the dynamic boundary condition at the earth's surface. (the sum of tractions at the surface is equal to zero.) On the other hand, a true incident angle is related to an apparent velocity as follows:

$$Vap = \frac{Vp}{\sin i} = \frac{Vs}{\sin j}.$$

For example, suppose we observe a wave with its apparent velocity of 6.0 km/s:

$i = 41.8^{o}, j = 22.6^{o}$ when Vp = 4.0 km/s and Vs = 2.3 km/s (Vp/VS = 1.74).

$i = 56.4^{o}, j = 28.8^{o}$ when Vp = 5.0 km/s and Vs = 2.9 km/s (Vp/Vs = 1.72).

These results show that i is approximately equal to $2j$ so that we can roughly regard i' as i.

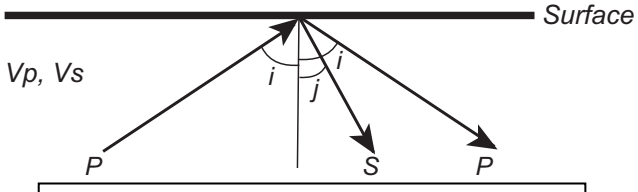

Fig. 3.3-3. Reflection and Incident Angles.

3.3 Phase Identification

Applying this method to observed phases, we can identify the type of phases.

3.3.1 Detection of initial S wave

It is sometimes very difficult to find the onset of an *S* wave, because an *S*-to-*P* converted phase arrives earlier than the *S* wave. However, if we analyze three-component seismograms, we can easily identify an *S* wave.

3.3.2 Identification of unknown phases

We sometimes observe predominant unknown phases. Comparing the direction of the particle motion of the unknown phase with those of *P* and *S* waves, we can tell the type of the analyzed phase. Therefore, this method is used in analyses of unknown phases. For example, Matsuzawa *et al*. (1986, 1990) analyzed later phases of microearthquakes and identified them as *P*-to-*S* and *S*-to-*P* converted waves at the subducting Pacific plate in northeastern Japan.

Exercise 3.1 Obtain the direction of the *P* wave approach and the apparent incident angle at KGN station (no. 11) in Fig. 2.6.

Exercise 3.2 Examples are shown in Figs. 3.4, 3.5, and 3.6. A predominant later phase exits between *P* and *S* waves at station ABSH of the Hurghada network in Egypt.

1. Plot particle motions of three phases, *P*, *X*, and *S* at ABSH (Fig. 3.6).
2. Obtain the direction of the *P* wave approach.
3. Obtain the apparent incident angle at ABSH.
4. Obtain the *P* velocity in the surface layer assuming the apparent velocity of the wave is 5.5 km/s.
5. Interpret what is the *X* phase.

References

Matsuzawa, T., Umino, N., Hasegawa, A., and Takagi, A., 1986, Upper mantle velocity structure estimated from PS-converted wave beneath the north-eastern Japan arc, Geophys. J. R. astr. Soc., 86, 767-787.

Matsuzawa, T., Kono, T., Hasegawa, A., and Takagi, A., 1990, Subducting plate boundary beneath the northeastern Japan arc estimated from SP converted waves, Tectonophysics, 181, 123-133.

Tsukuda, T., 1976, Microearthquake waveforms recorded at Tottori Microearthquake Observatory and their relation to hypocentral distributions and the upper-crustal structure, Bull. Disas. Prev. Res. Inst., Kyoto Univ., 6.

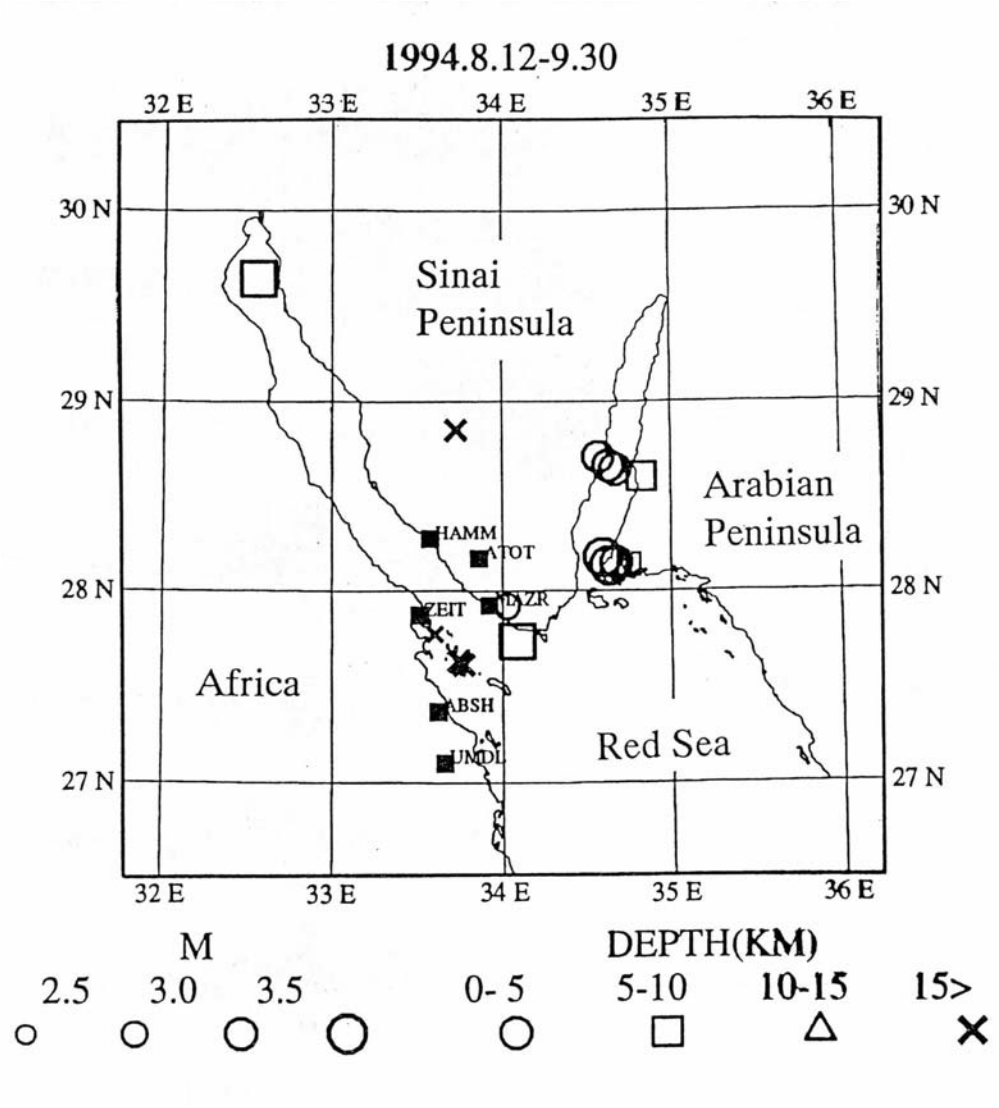

Fig. 3.4 Hurghada Seismic Network in Egypt as of Sept. 1994. Solid squares represent stations.

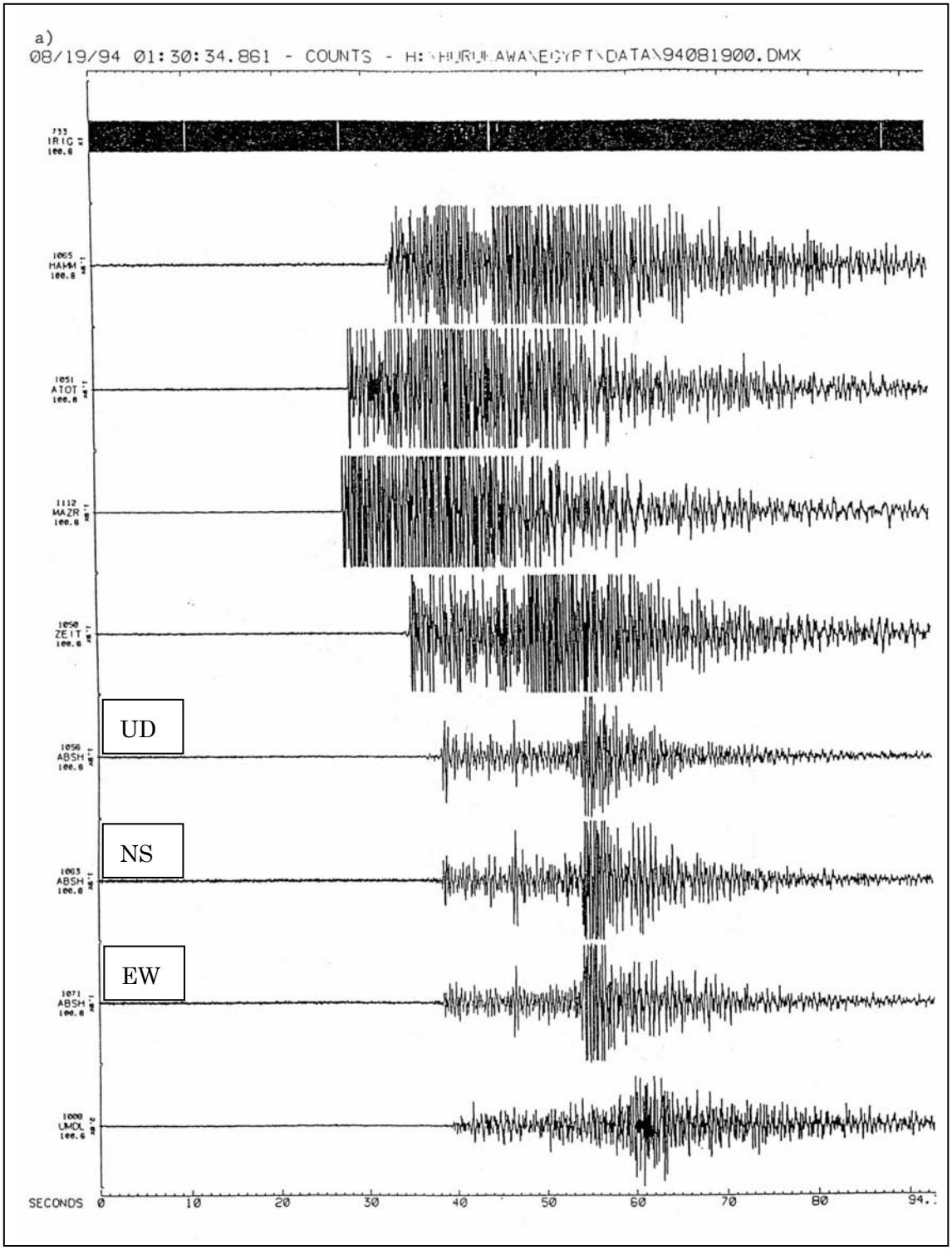

Fig. 3.5 Seismograms recorded at the Hurghada Seismic Network.

The epicenter of the earthquake is 28°07'N and 34°35'E.

a) Total waveforms at all stations.

b) Enlarged waveforms.

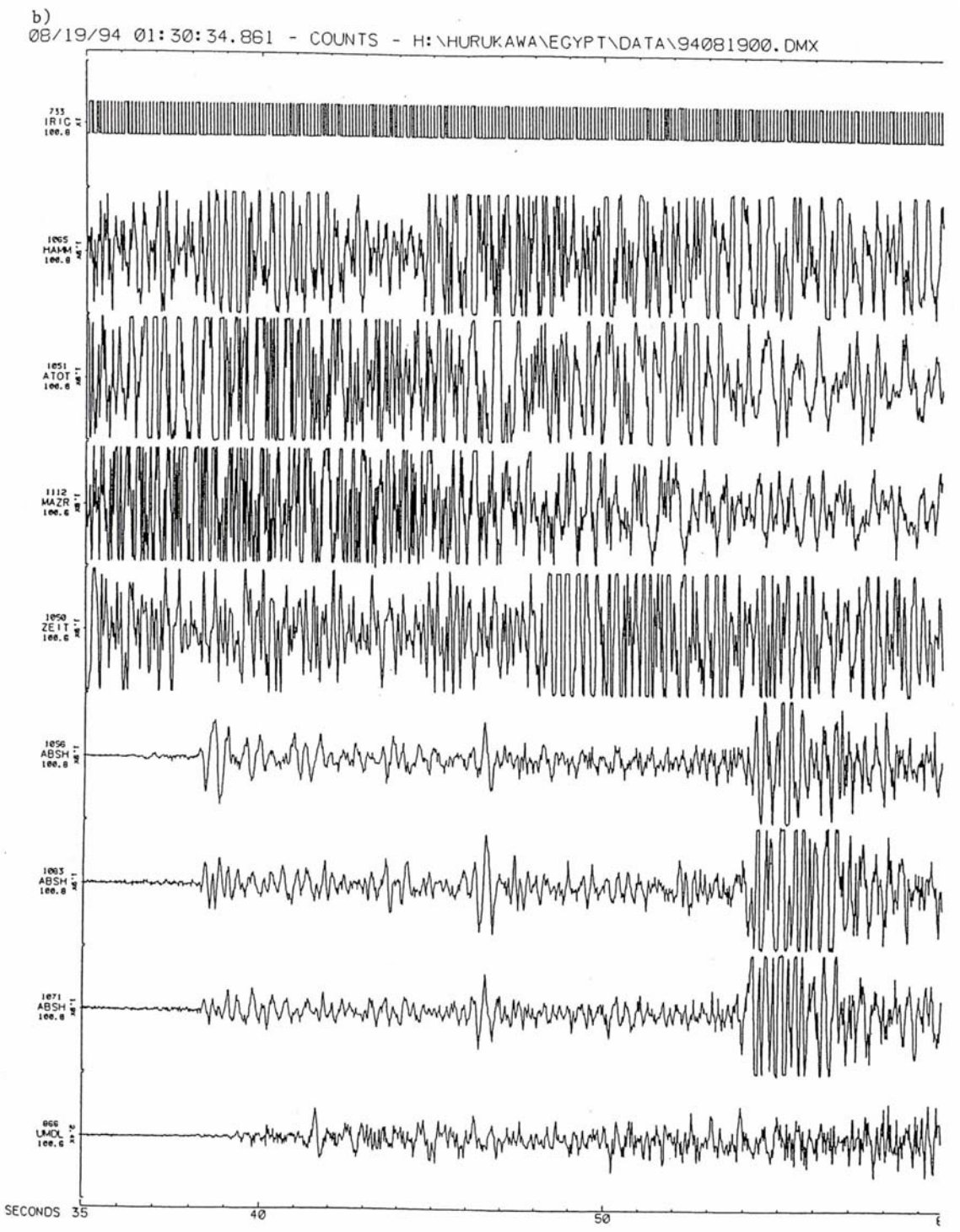

Fig. 3.5 (continued).

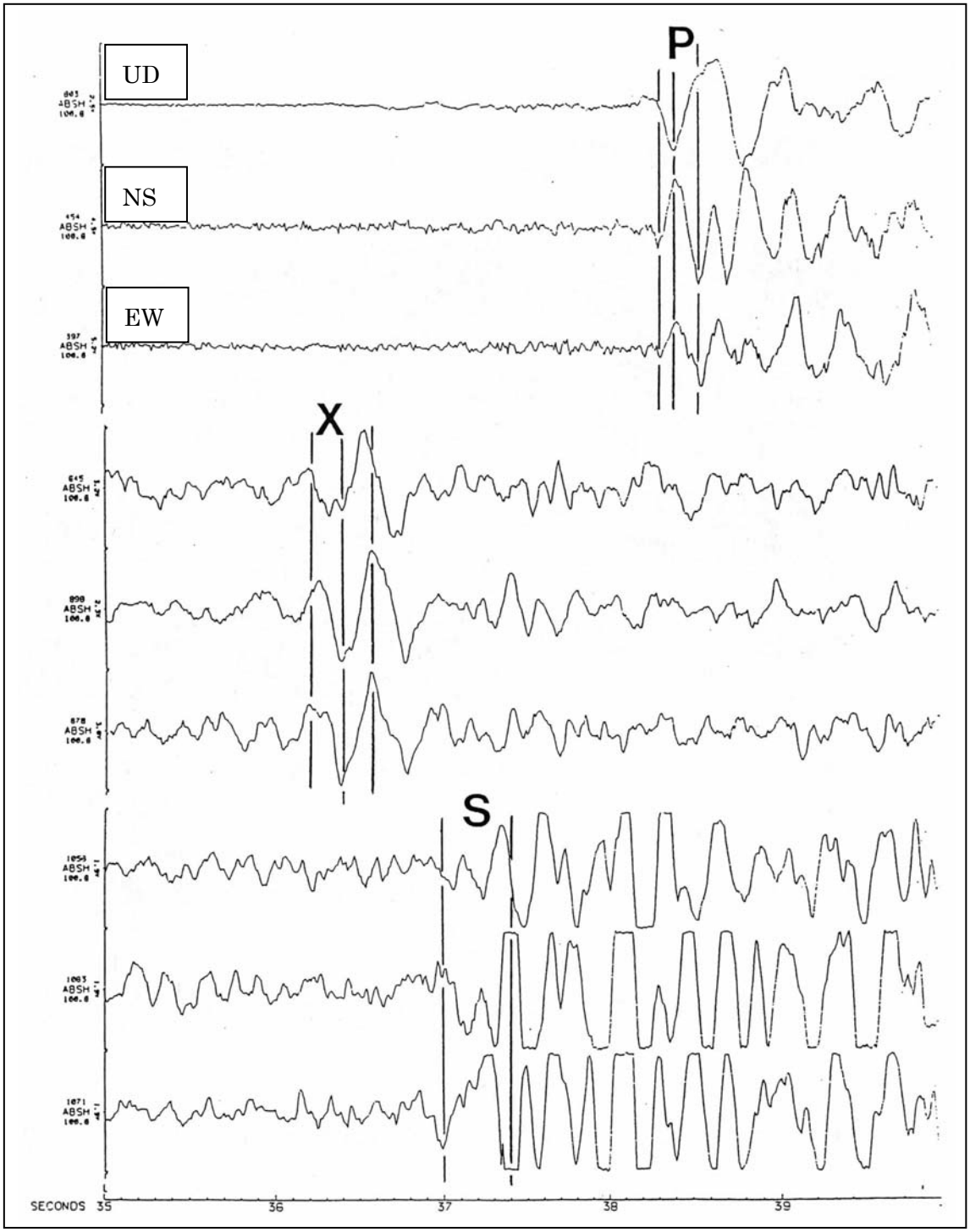

Fig. 3.6 Seismograms at station ABSH of the same event as Fig. 3.5.
Three-component seismograms of *P*, *X* (unknown phase), and *S* waves are shown..

Chapter 4 Apparent Velocity

Seismic waves of an earthquake arrive at stations on the earth's surface. Calculating the apparent velocity of seismic waves from travel-time differences at stations, we can tell approximately where the earthquake occurred.

4.1 Procedure

In the case where the distance between two stations is much less than the hypocentral distance, we can assume plane-wave incidence. Suppose there are two stations on the earth's surface and they are on a vertical plane that is parallel to the ray path of the seismic wave:

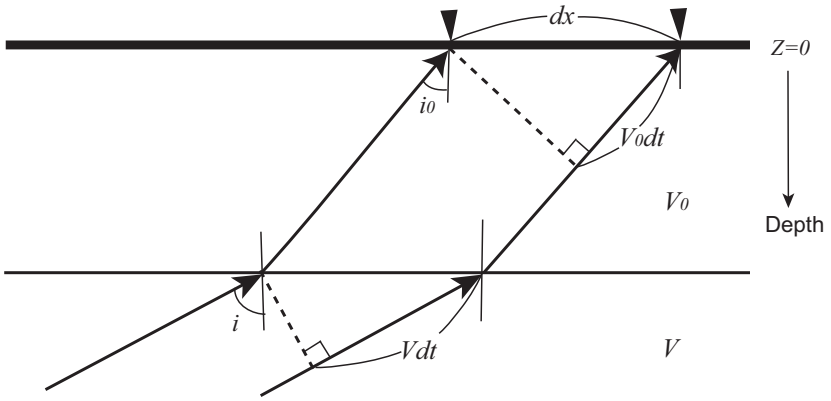

Fig. 4.1 Incidence of plane wave to the earth's surface.

Since a wave front is always perpendicular to ray paths, the relation between the difference of epicentral distances and the travel-time difference at two stations is as follows:

$$dx * \sin i_0 = V_o * dt$$

$$dx * \sin i = V * dt$$

Then

$$\frac{dx}{dt} = \frac{V_o}{\sin i_0} = \frac{V}{\sin i}.$$

The equation

$$\frac{V_o}{\sin i_0} = \frac{V}{\sin i}$$

is called *Snell's law*. The apparent velocity is defined as a velocity that the seismic wave travels apparently along the surface. Therefore, it is given as follows:

$$Vap = \frac{dx}{dt} = \frac{V}{\sin i} = \frac{1}{p}.$$

We call p the ray parameter. It is a constant along any given ray path. Note that an apparent velocity

is always greater than velocities in the media along the ray path from the source to the stations in laterally homogeneous media.

$$Vap \geqq V(z)$$

The apparent velocity and the direction of wave approach are calculated by travel-time data at a tripartite network or a seismic array. Note that the ray parameter in the spherical Earth is $p = r\sin i/V$, where r is the radial distance from the center of the Earth.

4.2 Tripartite

When the direction of wave approach is known, as is the above example, we can obtain the apparent velocity very easily. In order to know both the apparent velocity and the direction of wave approach, we need at least three stations. We use the tripartite network to know them. A tripartite is an observation system having three seismographs at the vertexes (apexes) of a triangle with a span of several hundred meters. Of course, we may make the span larger.

Suppose a seismic wave approaches three stations 1, 2, and 3 with apparent velocity *Vap* and direction of wave approach θ:

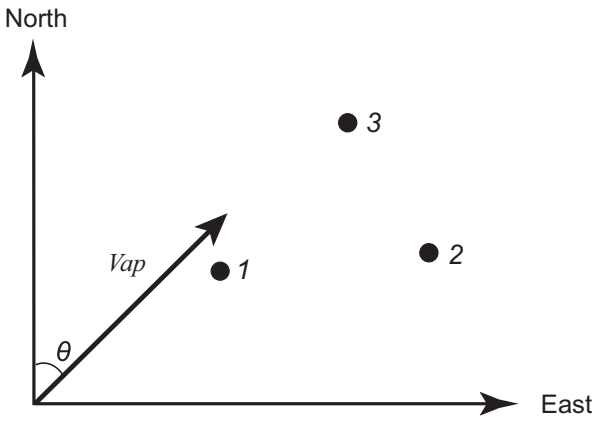

Fig. 4.2 Plane-wave incidence to tripartite with stations, 1, 2, and 3.

The following notations are used:

x_i, y_i: (x, y) coordinates of i-th station

t_i: Arrival time at i-th station

Vap: Apparent velocity

θ: Direction of wave approach (measured clockwise from the north)

Suppose the unit vector of the direction of wave approach is

$$\boldsymbol{u} = (\sin\theta, \cos\theta)$$

and the vector from station 1 to station 2 is

$$\boldsymbol{a} = (x_2 - x_1, y_2 - y_1).$$

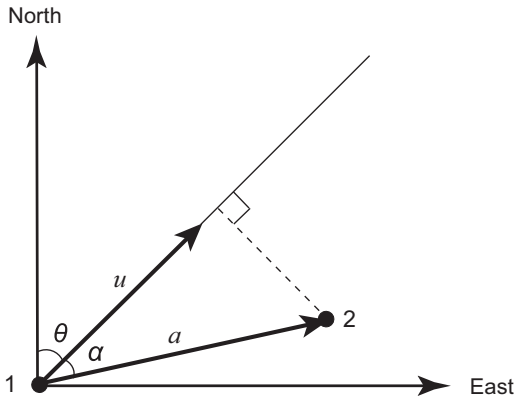

Fig. 4.3 Inner product of unit vector $\boldsymbol{u}$ and vector $\boldsymbol{a}$.

The inner product of these two vectors is

$$\boldsymbol{ua} = |\boldsymbol{u}||\boldsymbol{a}|\cos\alpha,$$

where α is the angle between vectors $\boldsymbol{u}$ and $\boldsymbol{a}$. Then

$$(x_2 - x_1)\sin\theta + (y_2 - y_1)\cos\theta = |\boldsymbol{a}|\cos\alpha.$$

Since

$$|\boldsymbol{a}|\cos\alpha = Vap(t_2 - t_1),$$

we get the following formula;

$$t_2 - t_1 = (x_2 - x_1)\frac{\sin\theta}{Vap} + (y_2 - y_1)\frac{\cos\theta}{Vap}. \tag{4.1}$$

In the same manner, we get the following formula from stations 1 and 3:

$$t_3 - t_1 = (x_3 - x_1)\frac{\sin\theta}{Vap} + (y_3 - y_1)\frac{\cos\theta}{Vap}. \tag{4.2}$$

Put

$$X = \frac{\sin\theta}{Vap}, \quad Y = \frac{\cos\theta}{Vap},$$

Equations (4.1) and (4.2) become

$$t_2 - t_1 = (x_2 - x_1)X + (y_2 - y_1)Y$$
$$t_3 - t_1 = (x_3 - x_1)X + (y_3 - y_1)Y,$$

Then

$$X = \frac{y_{31}t_{21} - y_{21}t_{31}}{x_{21}y_{31} - x_{31}y_{21}}, Y = \frac{x_{21}t_{31} - x_{31}t_{21}}{x_{21}y_{31} - x_{31}y_{21}},$$

where $x_{ij}=x_i-x_j$, etc. We can also write the above equations in matrix notation:

$$\begin{pmatrix} x_{21} & y_{21} \\ x_{31} & y_{31} \end{pmatrix}\begin{pmatrix} X \\ Y \end{pmatrix}=\begin{pmatrix} t_{21} \\ t_{31} \end{pmatrix}, \boldsymbol{AX}=\boldsymbol{T},$$

their solution is $\boldsymbol{X}=\boldsymbol{A}^{-1}\boldsymbol{T}$, that is

$$\begin{pmatrix} X \\ Y \end{pmatrix}=\frac{1}{x_{21}y_{31}-x_{31}y_{21}}\begin{pmatrix} y_{31} & -y_{21} \\ -x_{31} & x_{21} \end{pmatrix}\begin{pmatrix} t_{21} \\ t_{31} \end{pmatrix}=\frac{1}{x_{21}y_{31}-x_{31}y_{21}}\begin{pmatrix} y_{31}t_{21} & -y_{21}t_{31} \\ x_{21}t_{31} & -x_{31}t_{21} \end{pmatrix}$$

then

$$Vap=\frac{1}{\sqrt{X^2+Y^2}}$$

$$\theta=\tan^{-1}\frac{X}{Y}.$$ (In case that both X and Y are positive.)

When the number of stations is greater than three, we determine them by the least-squares method.

Examples:

1. Hurukawa and Hirahara (1980) analyzed later phases of a microearthquake and identified them as waves reflected at the subducting Philippine Sea plate in southwestern Japan.
2. Takeuchi *et al*. (1990) detected a source region of microtremors caused by submarine volcanic activity in the east off of the Izu peninsula, central Japan.
3. Hashizume *et al*. (1965) studied the accuracy of the tripartite method.

Exercise 4.1 Obtain apparent *P* and *S* wave velocities and the direction of *P* and *S* wave approaches of the event in Fig. 2.6 by using *P* and *S* times at three stations, SIZ, HKW, and OKB:

i	Code	x_i, km	y_i, km	tp_i, s	ts_i, s
1	SIZ	-61.1	-42.9		
2	HKW	-78.6	-44.8		
3	OKB	-68.2	-60.8		

4.3 Seismic Array

A seismic array is a set of seismographs distributed over an area of the earth's surface at spacing narrow enough that the signal waveform may be correlated between adjacent seismographs. Several examples are shown as follows:

Large Aperture Seismic Array (LASA); Montana, U.S.A.: There are 21 small subarrays in an area 200 km in diameter. Each subarray has 25 seismographs in a circle 7 km in diameter. (Capon, 1973)

Norwegian Seismic Array (NORSAR): It consists of 22 subarrays, each equipped with one three-component long-period and six vertical short-period instruments. The array diameter is around 110 km, while that of a subarray is approximately 8 km (Bungum *et al*., 1971). NORSAR was deployed originally to detect nuclear explosion experiments by the former USSR.

Matsushiro, Japan: This array is a backup system for the coming Tokai earthquake, operated by the Japan Meteorological Agency (JMA) at Matsushiro in Nagano Prefecture, central Japan.

The purposes of seismic array use are as follows:

1. To obtain the apparent velocity and the direction of wave approach.
2. To obtain signal enhancement on the basis of differences in the characteristics of wave propagation between the signal and noise. (Beam forming) (cf., Husebye *et al*., 1975, 1976)
3. To study detailed characteristics of wave propagation across an array.

4.4 Application of Apparent Velocity

4.4.1 Hypocenter determination

If an *S*-*P* time is known, the hypocentral distance can be calculated very easily as shown in Chapter 2. Then, we can roughly obtain a hypocenter.

4.4.2 Velocity-structure determination

4.4.2.1 Minimum apparent velocity method

Matumoto *et al*. (1977) obtained the crustal structure by using local earthquake data without knowledge of hypocenters in Managua, Nicaragua, and northern Costa Rica. They plotted apparent velocities against *S*-*P* times. Since the apparent velocity is always greater than velocities in the media along the ray path from the source to stations, the minimum apparent velocity at a certain *S*-*P* time represents the true velocity in media. We can then obtain the thickness of each layer from *S*-*P* times when the minimum apparent velocity changes. This is one of the simplest method for obtaining the velocity structure. Station corrections should be carefully corrected, however, to obtain a true velocity structure accurately.

4.4.2.2 $dT/d\Delta$ method (or apparent velocity method)

The structure of the Earth is obtained by the Herglotz-Wiechert method. However, it is very difficult to determine detailed structures, because the inevitable smoothing of travel-time data considerably obscures details. Direct measurement of apparent velocities $d\Delta/dT$ has a great

advantage in this respect over the ordinary travel-time method. Niazi and Anderson (1965) obtained the detailed upper-mantle *P*-velocity structure by using apparent velocities of first arrivals across the Tonto Forest array in Arizona. The epicenters ranged from 10^o to 30^o in distance. After their study many researchers, such as Johnson (1967), Kanamori (1967), Chinnery and Toksoz (1967), and Fukao (1977), obtained detailed upper and lower mantle *P*-velocity structures by the $dT/d\Delta$ method.

References

Bungum, H., Husebye, E. S., and Ringdal, F., 1971, The NORSAR array and preliminary results of data analysis, Geophys. J. R. astr. Soc., 25, 115-126.

Capon, J., 1973, Signal processing and frequency wavenumber spectrum analysis for a large aperture seismic array, Methods Compt. Phys., 13, 1-59.

Chinnery, M. A., Toksoz, M. N., 1967, P-wave velocities in the mantle below 700 km, Bull. Seismol. Soc. Am., 57, 199-226.

Fukao, Y., 1977, Upper mantle P structure on the ocean side of the Japan-Kurile Arc, Geophys. J. R. astr. Soc., 50, 621-642.

Hashizume, M., Oike, K. and Kishimoto, Y., 1965, On the accuracy of tripartite method, Bull. Disast. Prev. Res. Inst., Kyoto Univ., 87, 7-29.

Hurukawa, N. and Hirahara, K., 1980, Structure of the Philippine Sea plate subducting beneath the Kii peninsula, Zisin (J. Seismol. Soc. Japan), 33, 303-316 (in Japanese with English abstract).

Husebye, E. S., King, D. W., and Haddon, R. A. W., 1976, Precursors to PKIKP and seismic wave scattering near the mantle-core boundary, J. Geophys. Res., 81, 1870-1882.

Husebye, E. S., Haddon, R. A. W., and King, D. W., 1977, Precursors to P'P' and upper mantle discontinuities, J. Geophys., 43, 535-543.

Johnson, L. R., 1967, Array measurements of P velocities in the upper mantle, J. Geophys. Res., 72, 6309-6325.

Kanamori, H., 1967, Upper mantle structure from apparent velocities of P wave recorded at Wakayama Micro-earthquake Observatory, Bull. Earthq. Res. Inst., Tokyo Univ., 45, 657-678.

Matumoto, T, Ohtake, M., Lathan, G., and Umana, J., 1977, Crustal structure in southern central America, Bull. Seism. Soc. Am., 67, 121-134.

Niazi, M., and Anderson, D. L., 1965, Upper mantle structure of western north America from apparent velocities of P waves, J. Geophys. Res., 70, 4633-4640.

Takeuchi, F., Shibutani, T., Ohkura, T., Watanabe, K., Hirano, N., Matsumura, K., and Nishigami, K., 1990, Observation of micro tremors after the 1989 eruption off east coast of Izu Peninsula, Annuals, Disas. Prev. Res. Inst., Kyoto Univ., 33, 13-21 (in Japanese with English abstract).

Chapter 5 Hypocenter Determination

The most fundamental parameters of an earthquake are the hypocenter and the origin time. The hypocenter and the origin time are a location (longitude, latitude, and depth) of the earthquake where it occurred and the time when the earthquake occurred. Since we analyze earthquakes observed in a local network, the hypocenter is represented by Cartesian coordinates (x, y, z) here. The term hypocenter sometimes means both the location and the origin time of the earthquake. In the case of hypocenter determination, we usually determine both. We use *P*- and *S*-wave arrival times at seismic stations in hypocenter determination. There are several methods for determining the hypocenter of an earthquake. Here, I classify them as graphical and calculative methods.

5.1 Graphical Method

There are several ways to locate an earthquake graphically without using a computer or calculator. Hypocentral distances are necessary to locate the earthquake graphically. Since hypocentral distances are calculated using both *P*- and *S*-wave arrival times (Section 2.3), it is not possible to know the hypocenter without *S* time(s). First, we obtain the origin time graphically by a Wadati diagram (Sections 2.1 and 2.2). Second, the location is obtained by following methods.

5.1.1 Case 1: Three stations

It is very easy to obtain the hypocenter graphically when *S*-*P* times at three stations are available. This method uses only a ruler and compass. Since we use hypocentral distances in this graphical method, we must obtain these before using this method.

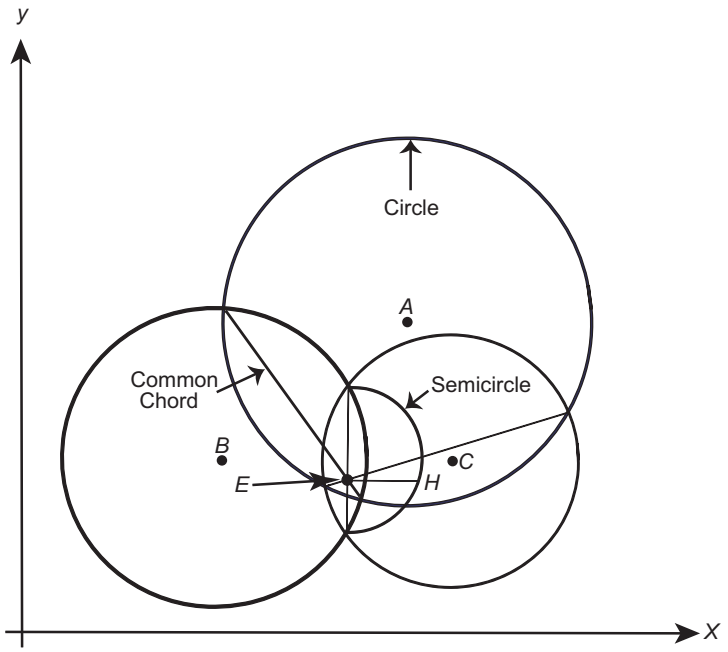

Fig. 5.1 Graphical method of hypocenter determination using three stations, A, B, and C.

The method is as follows:

1. Draw circles with three stations, A, B, and C, as centers and hypocentral distances as radii.
2. Draw two common chords. A point of intersection, E, is the epicenter of the earthquake.
3. Draw a semicircle of which diameter is one of the common chords. Draw a straight line that passes through E and is perpendicular to the common chord. Suppose a point of intersection of the straight line and the semicircle is H. Distance EH is a focal depth.

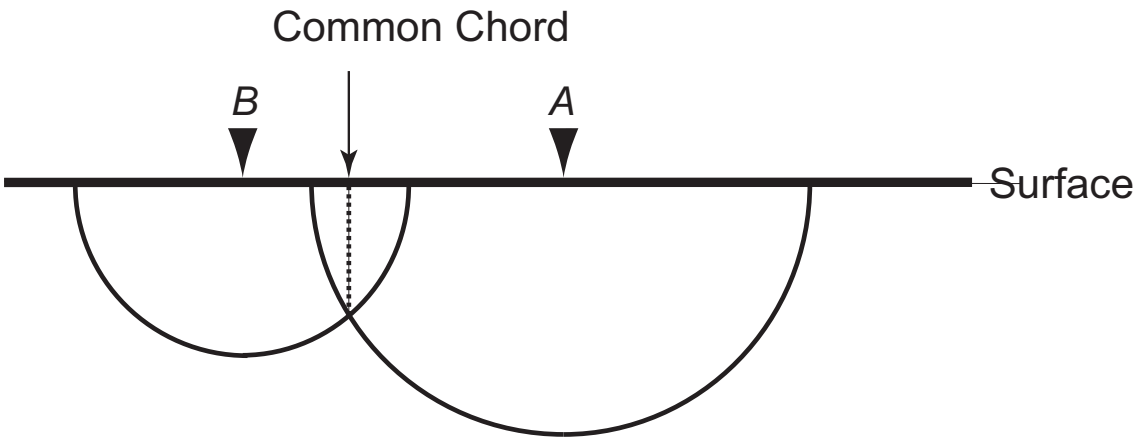

Fig. 5.2 Vertical cross section along stations A and B in Fig. 5.1.

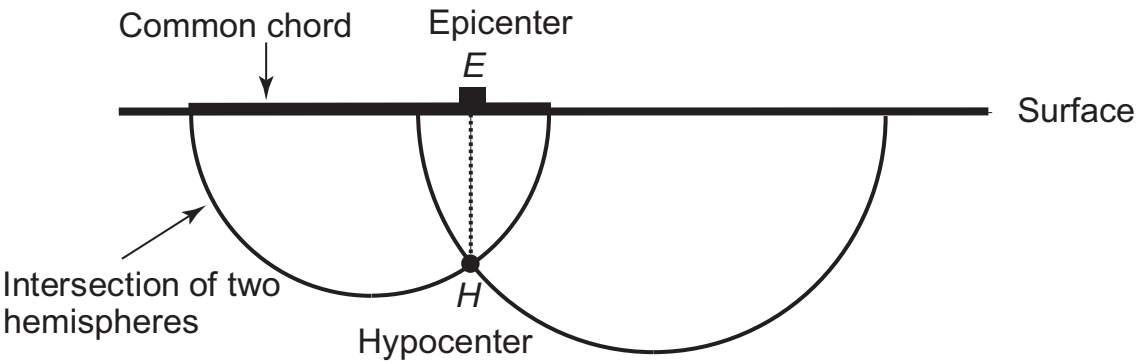

Fig. 5.3 Vertical cross section along one common chord in Fig. 5.1.

Therefore, if we have three stations, we can obtain the hypocenter of the earthquake graphically. This is the most primitive method to locate an earthquake. There are two ways to obtain the hypocentral distance, which are used in the above method.

5.1.1.1 Three *S-P* times

The hypocentral distance of each station is calculated by the following *Oomori formula* in equation (2.9):

$$D = k * Tsp, \tag{5.1}$$

where k and Tsp are the *Oomori coefficient* and *S-P* time, respectively, and from equation (2.8)

$$k = \frac{Vp}{\frac{Vp}{Vs} - 1},$$

given in Chapter 2, where Vp and Vs are the *P*- and *S*-wave velocities, respectively. This method is especially useful in the case where the absolute time is unknown.

Exercise 5.1 Obtain the hypocenter of the earthquake analyzed in Chapter 2 graphically using 3 of the 12 stations shown in Fig. 2.6 and assuming k = 8. Compare it to the routine hypocenter shown in the same figure.

If we use this simple equation in Exercise 5.1, that is

$$D = 8Tsp,$$

we can obtain the rough epicenter or hypocenter very easily as follows: Suppose seismograms are recorded on papers with a speed of 8 mm/s and a reduced scale of the station map is 1:1,000,000, we can obtain the epicenter using a compass and no ruler; 8 mm on the seismogram corresponds to 1 s and 1 s to 8 km in hypocentral distance, that is, 1 mm on the seismogram corresponds to 1 km on the map.

1 mm : 1 km = 1 : 1,000,000

The reduced scale is the same as that of the map.

5.1.1.2 Three *P* times

When *S* arrivals at only one or two stations are available, we cannot use the previous method. However, the hypocentral distance is calculated assuming the origin time of this event obtained by a Wadati diagram. The hypocentral distance is represented by the following formula;

$$D = Vp * Tpo,$$

where Vp and Tpo are *P*-wave velocity and travel time, respectively.

5.1.2 Case 2: Two stations

5.1.2.1 One-component seismograph

We obtain the possible region of the hypocenter as follows:

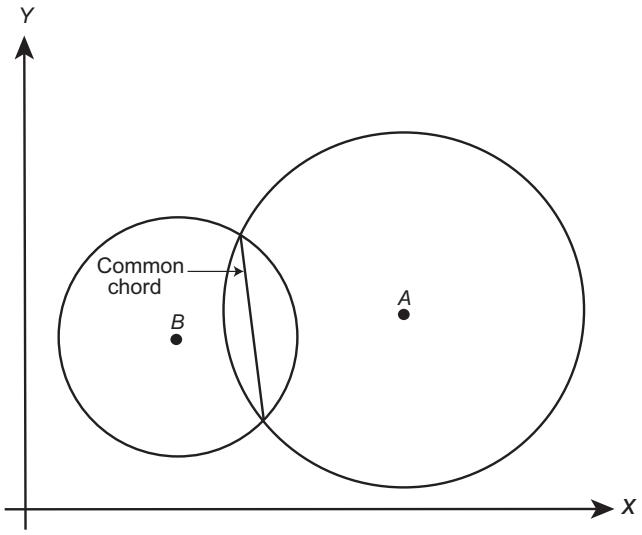

Fig. 5.4 Graphical method of hypocenter determination for stations A and B.

The method is as follows:

1. Draw circles with stations as centers and hypocentral distances as radii.
2. Draw a common chord.

The common chord is the possible area of the epicenter.

5.1.2.2 Two horizontal-component seismographs

We can obtain the horizontal particle motion of the initial *P* wave parallel to the direction to the epicenter (Chapter 3). Cross point E of one or two directions at two stations and the common chord obtained above is the epicenter. A focal depth is obtained in the same manner as that in case *1*.

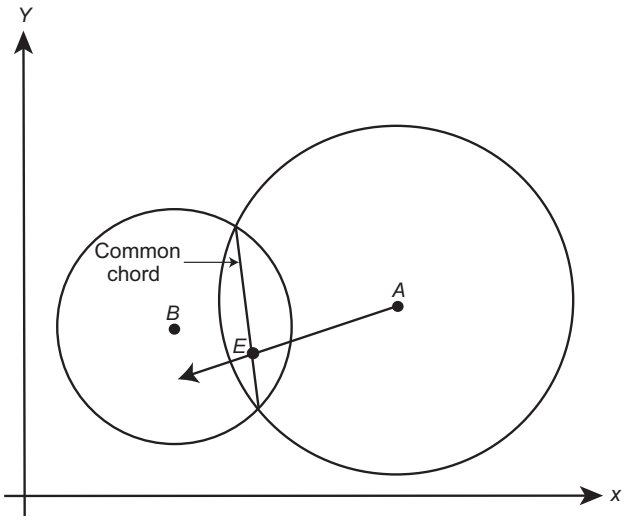

Fig. 5.5 Graphical method of hypocenter determination for two stations with two horizontal-component seismographs.

5.1.2.3 Three-component seismographs (one vertical and two horizontal)

In addition to the above method we can obtain the hypocenter of the earthquake with the particle motion given in Chapter 3.

5.1.3 Case 3: One Station

5.1.3.1 One component seismograph

It is not possible to determine the hypocenter in this case. We can only estimate the hypocentral distance from the following equation (5.1):

$$D = k * Tsp.$$

5.1.3.2 Two horizontal-component seismographs

In addition to the hypocentral distance, we can determine the direction and the direction opposite to the epicenter from the horizontal particle motion of the initial *P* wave. We can therefore determine two candidates of the epicenter.

5.1.3.3 Three-component seismographs

We can obtain the hypocenter of the earthquake observed at a three-component station. The hypocenter is estimated by the particle motion of the initial wave and the *S*-*P* time as described in Chapter 3.

5.2 Calculative Method

5.2.1 Homogeneous media

If the origin time is known, we can very easily calculate the hypocenter of an earthquake using *P* times at three stations assuming homogeneous media.

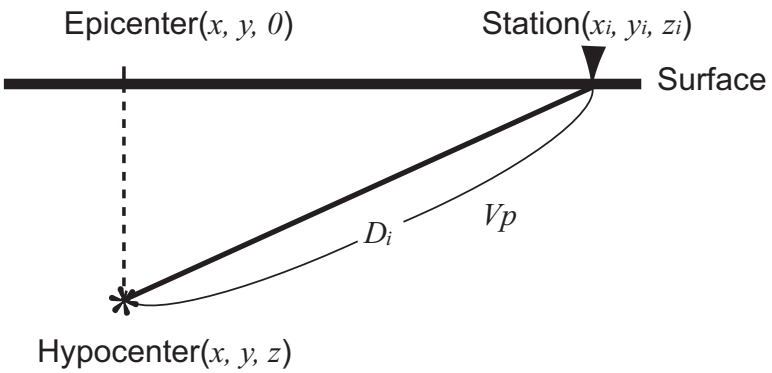

Fig. 5.6 Schematic cross section along the ray path in homogeneous media.

Suppose the following notation:

(x, y, z): Hypocenter (unknown)

Vp: P-wave velocity in media (given)

To: Origin time (given)

(x_i, y_i, z_i): Coordinate of i-th station; i=1, 2, 3 (given)

t_i: P wave arrival time at i-th station (observed)

D_i: Hypocentral distance at i-th station

A hypocentral distance at the i-th station is represented by Vp, To, (x, y, z), (x_i, y_i, z_i), and t_i as follows:

$$D_i^2 = (x_i - x)^2 + (y_i - y)^2 + (z_i - z)^2 = Vp^2 (t_i - To)^2 \qquad (i=1, 2, 3).$$

Since these are not linear equations of x, y, and z, it is difficult for us to solve these equations. Therefore, we modify them to linear equations of x, y, and z. Suppose that an approximate hypocenter is (x_0, y_0, z_0), and $x=x_0+dx$, $y=y_0+dy$, and $z=z_0+dz$, we can rewrite the above equations as follows:

$$(x_i - x_0 - dx)^2 + (y_i - y_0 - dy)^2 + (z_i - z_0 - dz)^2 = Vp^2 (t_i - To)^2 \quad (i=1, 2, 3)$$

If we ignore dx^2, dy^2 and dz^2, we can obtain the following linear equations for dx, dy, and dz:

$$\begin{aligned} &2(x_i - x_0)dx + 2(y_i - y_0)dy + 2(z_i - z_0)dz \\ &= (x_i - x_0)^2 + (y_i - y_0)^2 + (z_i - z_0)^2 - Vp^2 (t_i - To)^2 \end{aligned} \qquad (i=1, 2, 3)$$

These simultaneous linear equations of dx, dy, and dz enable us to easily solve these equations. There are several methods for solving simultaneous linear equations, such as elimination. Equations can be written in matrix notation as follows:

$$\boldsymbol{AX} = \boldsymbol{B},$$

where

$$\boldsymbol{A} = \begin{pmatrix} 2(x_1 - x_0) & 2(y_1 - y_0) & 2(z_1 - z_0) \\ 2(x_2 - x_0) & 2(y_2 - y_0) & 2(z_2 - z_0) \\ 2(x_3 - x_0) & 2(y_3 - y_0) & 2(z_3 - z_0) \end{pmatrix}, \quad \boldsymbol{X} = \begin{pmatrix} dx \\ dy \\ dz \end{pmatrix},$$

$$\mathbf{B} = \begin{pmatrix} (x_1 - x_0)^2 + (y_1 - y_0)^2 + (z_1 - z_0)^2 - Vp^2 (t_1 - To)^2 \\ (x_2 - x_0)^2 + (y_2 - y_0)^2 + (z_2 - z_0)^2 - Vp^2 (t_2 - To)^2 \\ (x_3 - x_0)^2 + (y_3 - y_0)^2 + (z_3 - z_0)^2 - Vp^2 (t_3 - To)^2 \end{pmatrix}.$$

The solution to the above equation is

$$\boldsymbol{X} = \boldsymbol{A}^{-1}\boldsymbol{B} \quad \text{or} \quad \boldsymbol{X} = (\boldsymbol{A}'\boldsymbol{A})^{-1}\boldsymbol{A}'\boldsymbol{B},$$

where $\boldsymbol{A}'$ and $(\boldsymbol{A}'\boldsymbol{A})^{-1}$ are the transposed and the inverse matrices of $\boldsymbol{A}$ and $\boldsymbol{A}'\boldsymbol{A}$, respectively. This is also the least-squares solution of it when the number of stations is greater than three. Since we ignore dx^2, etc., we must repeat to solve the equation until (dx, dy, dz) become zero.

Exercise 5.2 Obtain the hypocenter of the following earthquake observed at three stations. Assume Vp = 6.0 km/s and use (x_1, y_1, 10.0) as the initial hypocenter (x_0, y_0, z_0). The origin time is To = 22.00 s.

Table 5.2 Coordinates of stations and arrival times.

Code	x_i, km	y_i, km	h_i, km	T_i, s
ASG	2.5	-20.7	0.4	26.93
HHR	6.9	26.1	0.6	27.85
SMB	-46.9	-9.2	0.2	29.82

We can easily extend this method to solve a fourth unknown To, which was given as a known in the above example. Moreover, the method is modified very easily. If the focal depth is known, you may fix it in hypocenter calculation.

5.2.2 Heterogeneous media

It is not possible to formulate theoretical travel times in actual three-dimensionally heterogeneous media, in general. We therefore use the Geiger's method in this case. Since we assume horizontally layered media in general, a theoretical travel time is a function of the epicentral distance and a focal depth of an earthquake.

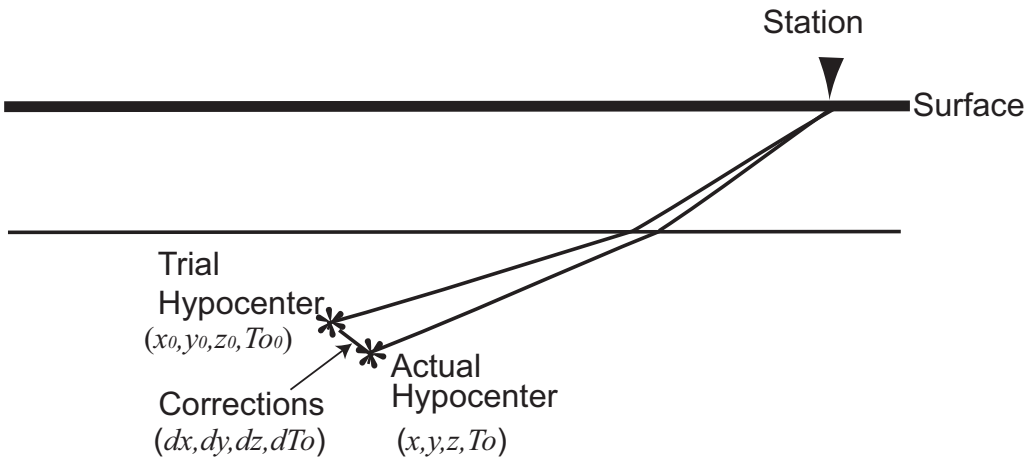

Fig. 5.7 Schematic vertical cross section along the ray path in horizontally layered media.

Suppose (x, y, z), To, (x_0, y_0, z_0), and To_0 are the actual hypocenter, the actual origin time, the trial hypocenter and the trial origin time, respectively, as in the definition in Section 5.2.1. Corrections to the trial hypocenter are $dx = x\text{-}x_0$, $dy = y\text{-}y_0$, $dz = z\text{-}z_0$, and $dTo = To\text{-}To_0$. Since we can calculate the theoretical travel time, the travel-time residual (O-C or observed minus calculated travel time) at each station is given by the following equation:

$$(O-C)_i = (t_i - To_0) - T_i = \frac{\partial t_i}{\partial x}dx + \frac{\partial t_i}{\partial y}dy + \frac{\partial t_i}{\partial z}dz + dTo, \qquad (5.2)$$

where t_i and T_i are the arrival time and the calculated travel time at the i-th station, respectively, and suffix i represents the i-th station (i=1, 2, ...). Since three coefficients ($\partial t_i /\partial x$, $\partial t_i /\partial y$, $\partial t_i /\partial z$) are easily calculated from the travel-time table, we can obtain four unknowns (dx, dy, dz, dTo) by the least-squares method as follows:

Sum of $(O\text{-}C)^2 \rightarrow$ Min

The improved hypocenter and improved origin time are then given by x_0+dx, ... and To_0+dTo. We use these values as our new trial hypocenter and origin time. We repeatedly solve this equation until these four unknowns become zero.

References on hypocenter determination are Lee and Stewart (1981) and Aki and Richards (1980).

5.2.3 Example of Geiger's method

Consider a 2-D problem for simplicity. Suppose a hypocenter and stations are on the x-z plane. Since the origin time is easily obtained using a *Wadati diagram*, unknowns of the problem are x and z coordinates of the hypocenter. Therefore, equation (5.2) is modified as follows:

$$(O-C)_i = (t_i - To) - T_i = \frac{\partial t_i}{\partial x}dx + \frac{\partial t_i}{\partial z}dz \qquad (5.3)$$

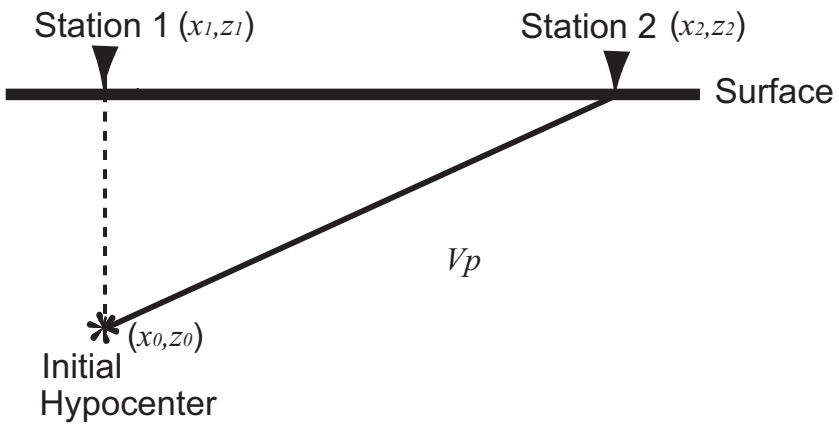

Fig. 5.8 Stations and initial hypocenter in 2-D case.

Suppose

Vp = 6.00 km/s (assumed)

To = 12.00 s (given)

x_1 = 0.0 km (given)

z_1 = 0.0 km (given)

x_2 = 15.0 km (given)

z_2 = 0.0 km (given)

t_1 = 13.41 s (observed)

t_2 = 14.13 s (observed)

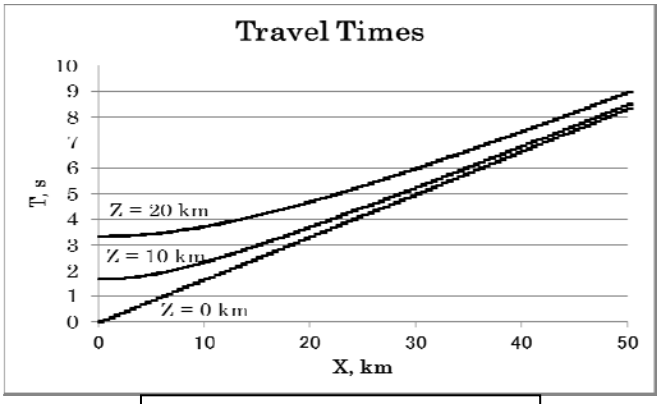

Fig. 5.8-2. Travel-time curves.

The calculated (theoretical) travel times at two stations are easily obtained as follows:

$$T_i = \sqrt{(x_i - x_0)^2 + (z_i - z_0)^2} \,/\, \mathrm{Vp}$$

Coefficients (partial derivatives of travel times with respect to x and z) are as follows, although not strict but easiest:

$$\partial t_i / \partial x = \sqrt{(x_i - (x_0 + 1))^2 + (z_i - z_0)^2} \,/\, \mathrm{Vp} - T_i$$

$$\partial t_i / \partial z = \sqrt{(x_i - x_0)^2 + (z_i - (z_0 + 1))^2} \,/\, \mathrm{Vp} - T_i$$

Where i = 1 and 2. (Difference between a travel time for the initial hypocenter and that at a point 1 km east or deep from the initial hypocenter.)

1. Iteration 1

Since the seismic wave arrived at station 1 first, we assume the following approximate (initial) hypocenter:

$x_0 = x_1$ = 0.00 km

z_0 = 10.00 km

Then,

$$T_1 = \sqrt{0^2 + 10^2} \,/\, 6.00 = 1.67s$$

$$T_2 = \sqrt{15^2 + 10^2} \,/\, 6.00 = 3.00s\,.$$

Equation (5.3) becomes as follows:

$$(O - C)_1 = (13.41 - 12.00) - 1.67 = 1.41 - 1.67 = -0.26 = \frac{\partial t_1}{\partial x} dx + \frac{\partial t_1}{\partial z} dz$$

$$(O-C)_2 = (14.13-12.00)-3.00 = 2.13-3.00 = -0.87 = \frac{\partial t_2}{\partial x}dx + \frac{\partial t_2}{\partial z}dz$$

Coefficients (partial derivatives of travel times with respect to x and z are as follows:

$\partial t_1/\partial x = 0.0083$ s/km

$\partial t_1/\partial z = 0.17$ s/km

$\partial t_2/\partial x = -0.14$ s/km

$\partial t_2/\partial z = 0.096$ s/km

cf. Suppose x increases 1 km with the fixing depth in calculation of partial derivatives for simplicity.

$$\partial t_1/\partial x = \sqrt{(0+1)^2+10^2}/6.00 - \sqrt{0^2+10^2}/6.00 = 1.6750 - 1.6667 = 0.0083 \text{ s/km}$$

Then, Equation (5.3) becomes as follows:

$$0.0083dx + 0.17dz = -0.26$$

$$-0.14dx + 0.096dz = -0.87$$

The following solution is derived:

dx = 5.00 km

dz = -1.77 km

The hypocenter is therefore as follows:

$x = x_0 + dx$ = 0.00 + 5.00 = 5.00 km

$z = z_0 + dz$ = 10.00 - 1.77 = 8.23 km

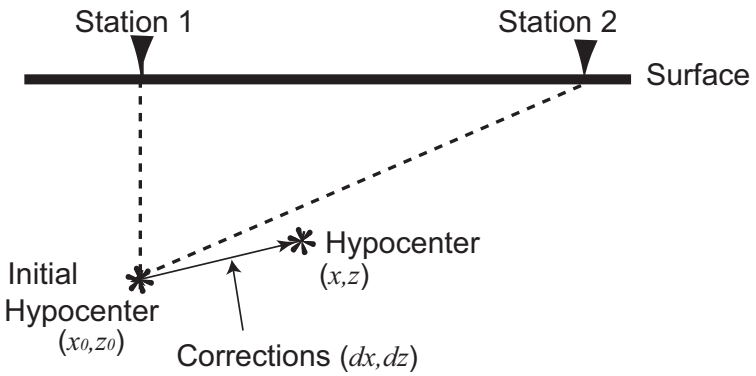

Fig. 5.9 Iteration 1.

Let's examine whether this solution satisfies the observed arrival times or not.

$$T_1 = \sqrt{5.00^2+8.23^2}/6.00 = 1.60s$$

$$T_2 = \sqrt{10.00^2+8.23^2}/6.00 = 2.16s\,.$$

Then

$$(O-C)_1 = 1.41 - 1.60 = -0.19$$
$$(O-C)_2 = 2.13 - 2.16 = -0.03$$

These are smaller than the original (*O*-*C*)s but not zeros. Therefore, we should repeat the calculation.

2. Iteration 2

Next, using solutions in iteration 1, we repeat the calculation:

x_0 = 5.00 km

z_0 = 8.23 km

Coefficients of *dx* and *dz* must be calculated again, because they depend on the location of the initial hypocenter. The calculated travel times and coefficients are as follows:

T_1 = 1.61 s

T_2 = 2.15 s

$\partial t_1 / \partial x = 0.093$ s/km

$\partial t_1 / \partial z = 0.145$ s/km

$\partial t_2 / \partial x = -0.126$ s/km

$\partial t_2 / \partial z = 0.110$ s/km

Equation (5.3) is as follows:

$$0.0093dx + 0.145dz = -0.19$$
$$-0.126dx + 0.110dz = -0.03$$

We get the following solution:

dx = -0.58 km

dz = -0.94 km

Therefore,

$x = x_0 + dx$ = 5.00 - 0.58 = 4.42 km

$z = z_0 + dz$ = 8.23 - 0.94 = 7.29 km.

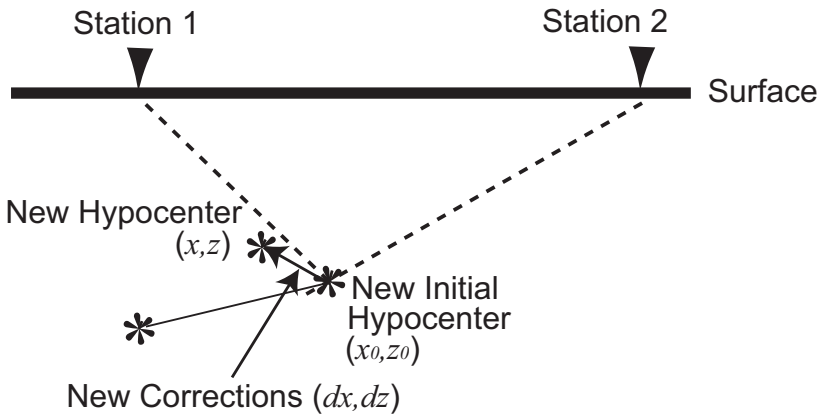

Fig. 5.10 Iteration 2.

Travel-time residuals for these solutions are as follows:

$(O\text{-}C)_1 = 1.41 - 1.42 = -0.01$

$(O\text{-}C)_2 = 2.13 - 2.14 = -0.01$

We can therefore find the root square sum of residuals decreases very rapidly:

Before iteration 1: 0.908 s

After iteration 1: 0.192 s

After iteration 2: 0.016 s

This process is repeated until corrections become zero.

Exercise 5.2 Changing initial hypocenter (x_0, z_0), calculate the hypocenter of the sample earthquake.

5.2.4 Computer programs

Several computer programs are available for hypocenter determination. The most famous is HYPO71PC, written by Lee and Valdes, is an IBM PC version of HYPO71 by Lee and Lahr (1975). (Section 5.3). Two more computer programs are HYPOINVERSE (Klein, 1978) and HYPOCENTER (Lienert *et al*., 1986). Differences in these three programs are described in Lienert *et al*. (1986).

5.2.5 Joint determination of hypocenters of many earthquakes

Certain techniques enable us to locate many earthquakes simultaneously. These methods were developed to improve hypocenter accuracy. Because of lateral heterogeneity of the actual Earth, an assumption of the horizontally layered model is not adequate to obtain precise location of earthquakes. We therefore define a station correction as follows:

A station correction is a travel-time difference between the assumed velocity structure and the actual one. It corrects a travel-time anomaly caused by the lateral heterogeneity. It is sometimes called a station delay. For example, suppose a station is located on a sedimentary layer with a low velocity that is different from other stations. A travel time at this station will be delayed compared with other stations on hard rock. This delay time should be corrected before hypocenter determination in order to obtain the correct earthquake location.

5.2.5.1 Joint hypocenter determination (JHD)

This technique is a generalization of the Geiger's method to include station corrections for travel times as additional parameters to be determined from a group of earthquakes. Hypocenters of many earthquakes and station corrections are calculated simultaneously (Douglas, 1967; Freedman, 1967; Hurukawa and Imoto, 1992). We modify equation (5.2) as follows:

$$(O-C)_{ij} = (t_{ij} - To_{0j}) - T_{ij} = \frac{\partial t_{ij}}{\partial x_j} dx_j + \frac{\partial t_{ij}}{\partial y_j} dy_j + \frac{\partial t_{ij}}{\partial z_j} dz_j + dTo_j + dS_i$$

where t_{ij} and T_{ij} are the arrival time and the calculated travel time of the j-th event at the i-th station, respectively. dS_i is a correction of a station correction at the i-th station. Other notations are the same as Section 5.2.2, excluding suffix j.

5.2.5.2 Master event method

This is a method to determine the relative location of earthquakes to a master event. Travel-time differences between the master event and others at stations are used in this method (Dewey, 1972).

5.2.5.3 Modified JHD

When media is very heterogeneous and station coverage is not good, solutions by the conventional JHD method (Douglas 1967; Freedman 1967) are unstable and unreliable because of the trade-off between station corrections and focal depths of earthquakes. Therefore, modifying the JHD method, Hurukawa and Imoto (1990, 1992) developed a modified joint hypocenter determination (MJHD) method by using the following constraints:

$$\sum_{i=1}^{n} S_i D_i = 0, \quad \sum_{i=1}^{n} S_i \cos\theta_i = 0, \quad \sum_{i=1}^{n} S_i \sin\theta_i = 0, \quad \sum_{i=1}^{n} S_i = 0,$$

where S_i, D_i, θ_i, and n are the station correction at the i-th station, the distance between the i-th station and the center of the region, the azimuth to the i-th station from the center of the region, and a number of stations, respectively. Note that the last equation is used in the conventional JHD method, too. These conditions imply that a station correction is independent of both the distance and the azimuth from the center of the studied region to the station. Although this sacrifices absolute hypocenters, this makes the JHD method stable. The MJHD method will bring almost the same results as the master-event method (Dewey, 1972). The MJHD method, however, has the major advantage that it is not necessary to select a master event. This is very effective, especially in a case where no earthquakes are observed clearly at all stations.

5.2.5.4 Simultaneous inversion of hypocenters and velocity structure

This is also a generalization of the Geiger's method to include velocity structure:

Cf. 1-D: Crosson (1976a, b)

3-D: Aki and Lee (1976)

5.3 Travel-Time Table

In horizontally layered media, the travel-time is a function of the focal depth and the epicentral distance. We prepare the travel-time table for a given velocity structure model to reduce computational time in hypocenter determination. Although you will learn the method for calculation of travel times in other lectures, such as 'Crust and upper-mantle structure', 'Seismic prospecting', etc., I will show it briefly.

First, we calculate travel times of direct waves for a certain focal depth. We interpolate them at the equal interval, such as 1 km.

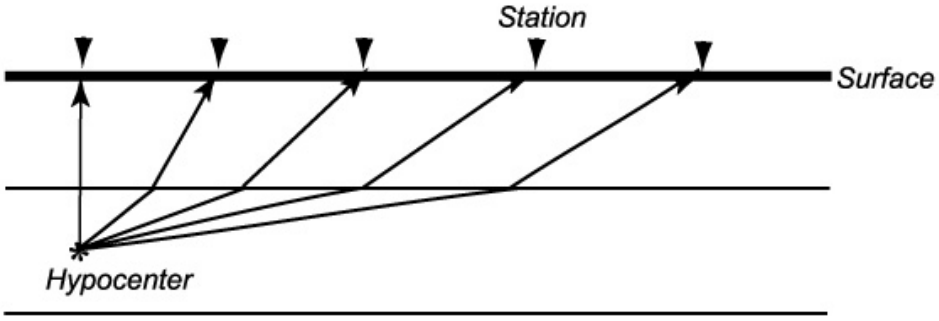

Fig. 5.11 Ray paths of direct waves.

Second, we calculate travel times of waves refracted at each layer boundary below the hypocenter for the same focal depth. We interpolate them in the same manner as direct waves.

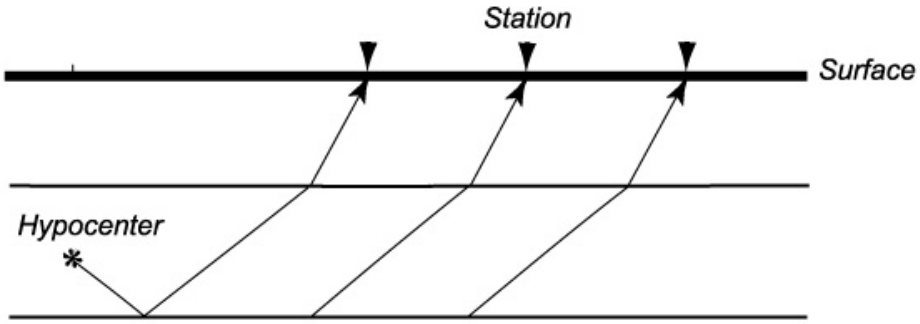

Fig. 5.12 Ray paths of refracted waves.

Since we use only first arrivals in hypocenter determination, we make the travel-time table of first arriving waves comparing travel times of different waves at a same epicentral distance. An example is shown in Tables 5.3 and 5.4. They are the *P*-wave velocity structure assumed in hypocenter determination and the travel-time table for the focal depth of 20 km, respectively.

Table 5.3 *P*-wave velocity structure.

No	*Vp*	*H*	*Z*
1	5.0	2.0	2.0
2	6.1	20.0	22.0
3	6.7	10.0	32.0
4	7.8	100.0	132.0

Vp; *P*-wave velocity in km/s

H; Thickness of the layer in km

Z; Depth to the bottom of the layer in km

Table 5.4 Travel-time table for focal depth of 20.0 km.

X	*T*	*I*	*W*
70.0	12.092	75.0	1
80.0	13.683	76.9	1
90.0	15.191	114.4	3
100.0	16.683	114.4	3
110.0	18.176	114.4	3
120.0	19.468	128.6	4
130.0	20.750	128.6	4

X; Epicentral distance in km

T; Travel time in sec

I; Emergent angle in deg

W; Wave type

= 1; Direct wave

= 2, .. Waves refracted from the top of the *W*-th layer

Emergent angles listed in Table 5.4 are used for determining focal mechanisms of earthquakes. You will learn how to obtain focal mechanisms of earthquakes in other lectures.

5.4 Conversion of (λ, φ) to (x, y)

When we calculate hypocenters of local earthquakes observed in a local network, we use Cartesian coordinates (x, y) instead of longitude λ and latitude φ. We must therefore convert λ and φ to x and y.

5.4.1 Calculation of epicentral distance and azimuth

The epicentral distance, the distance between the epicenter of an earthquake and a station, is measured along a great circle that passes through both the epicenter and the station. We calculate

them using spherical trigonometry with a slight modification (from Yoshii, 1987).

Suppose the following notation:

λ_E, φ_E: Longitude and latitude of epicenter

λ_S, φ_S: Longitude and latitude of station

θ_E: Azimuth to station from epicenter (measured from north to east)

θ_S: Azimuth to epicenter from station (measured from north to east)

Δ: Angular distance (Epicentral distance) in radian

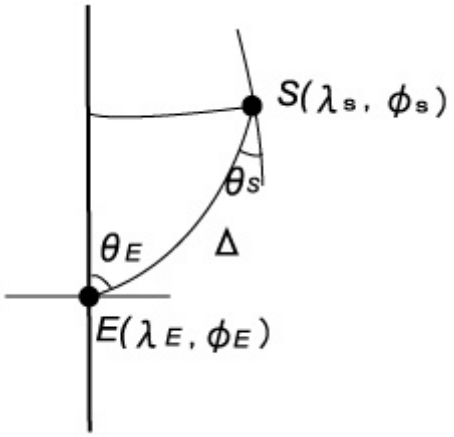

Fig. 5.13 Angular distance and azimuths of epicenter E and station S.

An epicentral distance is represented as follows:

$$\sin\frac{\Delta}{2} = \frac{\sqrt{(A_E - A_S)^2 + (B_E - B_S)^2 + (C_E - C_S)^2}}{2}$$

where

$$A_E = \cos\varphi_E \cos\lambda_E$$
$$A_S = \cos\varphi_S \cos\lambda_S$$
$$B_E = \cos\varphi_E \sin\lambda_E$$
$$B_S = \cos\varphi_S \sin\lambda_S$$
$$C_E = \sin\varphi_E$$
$$C_S = \sin\varphi_S$$

Two azimuths are represented as follows:

$$\cos\theta_E = \frac{\sin\varphi_S \cos\varphi_E - \cos\varphi_S \sin\varphi_E \cos(\lambda_S - \lambda_E)}{\sin\Delta}$$

$$\cos\theta_S = \frac{\sin\varphi_E \cos\varphi_S - \cos\varphi_E \sin\varphi_S \cos(\lambda_E - \lambda_S)}{\sin\Delta}$$

Since the angular distance should be measured against the center of the earth, we should use the

geocentric latitude instead of the geographical latitude. The conversion formula is as follows:

$$\tan\varphi = (1 - e^2)\tan\varphi'$$

where φ: Geocentric latitude

φ': Geographical latitude

e: Eccentricity of the ellipsoid of the earth

We obtain the epicentral distance in km from the angular distance by multiplying the radius of the Earth. It is sufficient to use the average of three axes of the Earth, 6,371 km, in general. However, if we use the following geocentric radius in this calculation, the result is very accurate, especially when the epicentral distance is short:

$$\rho = a(1 - \frac{1}{2}e^2 \sin^2\varphi' + \frac{1}{2}e^4 \sin^2\varphi' - \frac{5}{8}e^4 \sin^4\varphi'),$$

where a and φ' are the radius of the Earth at the equator and the average geographical latitude at the epicenter and station. Since the reference ellipsoid is the Bessel ellipsoid in Japan, we should use the following constants of the ellipsoid:

a = 6,377.397155 km

e^2 = 0.0066743722

5.4.2 Calculation of (x, y) station coordinate

We use station coordinate (x, y) instead of (λ_S, φ_S) with respect to the origin of coordinate (λ_0, φ_0). Suppose

λ_S, φ_S: Longitude and latitude of station

λ_0, φ_0: Origin of (x, y) coordinate in degrees

x,y: (x, y) coordinate in kilometers.

If we suppose that origin (λ_0, φ_0) correspond to (λ_E, φ_E) in Section 5.4.1, x and y are represented as follows:

$$x = \Delta\rho \sin\theta_E$$

$$y = \Delta\rho \cos\theta_E$$

5.5 HYPO71PC

IASPEI Seismological Software Library

The International Association of Seismology and Physics of the Earth's Interior (IASPEI) is a non-profit professional association dedicated to furthering the knowledge of seismology and solid-earth geophysics. In 1988, IASPEI established a Working Group on Personal Computers to promote the sharing of seismological software. This Working Group is chaired by W. H. K. Lee and includes the following members: .....

Under the auspices of the IASPEI Working Group on Personal Computers and in

collaboration with the Seismological Society of America (SSA), a series of seismological software volumes for IBM-compatible personal computers are being published under the editorship of W. H. K. Lee and F. Scherbaum. The editorial board is chaired by Hiroo Kanamori and includes the following members: ..... (from IASPEI leaflet, Sept. 7, 1994)

IASPEI Software Library Volume 1 (published in 1989) contains programs for real-time seismic data acquisition, processing, and analysis. HYPO71PC by Lee and Valdes (1989) is the program use for earthquake location in this volume. It is an IBM PC version of HYPO71 by Lee and Lahr (1975), which is the most popular computer program for determining hypocenters of local earthquakes in the world.

References

Aki, K. and Lee, W. H. K., 1976, Determination of three-dimensional velocity anomalies under a seismic array using first P arrival times from local earthquakes. Part 1. A homogeneous initial model., J. Geophys. Res., 81, 4381-4399.

Aki, K. and Richards, P., 1980, Quantitative Seismology, Vol. 2, Freeman.

Crosson, R. S., 1976a, Crustal structure modeling of earthquake data, 1, Simultaneous least squares estimation of hypocenter and velocity parameters, J. Geophys. Res. 81, 3036-3046.

Crosson, R. S., 1976b, Crustal structure modeling of earthquake data, 2, Velocity structure of the Puget Sound region, Washington, J. Geophys. Res. 81, 3047-3053.

Dewey, J. W., 1972, Seismicity and tectonics of western Venezuela, Bull. Seism. Soc. Am., 62, 1711-1751.

Douglas, A., 1967, Joint epicenter determination, Nature, 215, 47-48.

Freedman, H. W., 1967, A statistical discussion of P residuals from explosions, Part 2, Bull. Seism. Soc. Am., 57, 545-561.

Hurukawa, N. and Imoto, M., 1990, Fine structure of an underground boundary between the Philippine Sea and Pacific plates beneath the Kanto district, Japan, Zisin (J. Seismol. Soc. Jpn.), 43, 413-429 (in Japanese with English abstract).

Hurukawa, N. and Imoto, M., 1992, Subducting oceanic crusts of the Philippine Sea and Pacific plates and weak-zone-normal compression in the Kanto district, Japan, Geophys. J. Int., 109, 639-652.

Klein, F. W., 1978, Hypocenter location program HYPOINVERSE Part 1: Users guide to versions 1,2,3 and 4, USGS Open File Report, 78-694.

Lee, W. H. K. and Lahr, J. C., 1975, HYPO71 (revised): A computer program for determining hypocenter, magnitude and first motion pattern of local earthquakes, USGS Open File Report, 1-116.

Lee, L. H. K. and Stewart, S. W., 1981, Principles and Applications of Microearthquake Networks, Academic Press.

Lienert, B. R., Berg, E., and Frazer, N., 1986, HYPOCENTER: An earthquake location method using centered, scaled, and adaptively damped least squares, Bull. Seism. Soc. Am., 76, 771-783.

Lee, W. H. K. and Lahr, J. C., 1972, HYPO71: A computer program for determining hypocenter, magnitude and first motion pattern of local earthquakes, USGS Open File Report, 75-311.

Lee, W. H. K. and Valdes, C. M., 1989, User Manual for HYPO71PC, in IASPEI Software Library Volume 1. Toolbox for Seismic Data Acquisition, Processing and Analysis, Part III. Off-line Data Analysis, Edited by W. H. K. Lee, Published by International Association of Seismology and Physics of the Earth's Interior (IASPEI) in collaboration with Seismological Society of America, 203-236.

Yoshii, 1987, Calculation of Epicentral Distance and Azimuth, Encyclopedia of earthquake, edited by Utsu, Asakura Shoten, 48-49 (in Japanese).

Chapter 6 Magnitude

We use the following two types of magnitude in microearthquake observatories in general, and these are empirical formulas that fit the original Richter's magnitude scale:

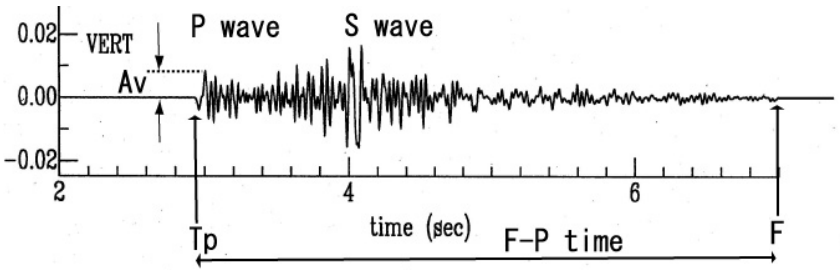

Fig. 6.1 Microearthquake waveform. The Unit of the vertical axis is cm/sec.

6.1 Velocity Amplitude Magnitude

Magnitude scales are usually defined by the displacement of the ground, because of original displacement seismographs. Since high-gain velocity seismographs are used in microearthquake observations in general, we use velocity amplitudes to obtain magnitudes. Watanabe (1971) proposed a formula to obtain magnitudes of microearthquakes using velocity amplitudes:

Watanabe's Formula

$$M = 1.18 \log A_v + 2.04 \log D + 2.94 \qquad \text{for } D<200 \text{ km}, \tag{6.1}$$

where A_V and D are the maximum velocity amplitude of the vertical-component seismograph in kine and the hypocentral distance in km, respectively. Since we use amplitudes of seismic waves in measuring magnitudes, we must know the correct value of sensitivities of seismographs and that of amplifications of the observation system.

Exercise 6.1 Calculate the velocity magnitude of the event shown in Fig. 6.1. You can use the maximum amplitude obtained in Exercise 1.1.

6.2 F-P Magnitude

This is a simplest magnitude scale. The duration time of the earthquake is used to obtain the magnitude of an earthquake:

$$M = a \log(F - P) + b \tag{6.2}$$

where

M: Magnitude

F: End time of seismic signal

F-P: *F-P* time (total duration of oscillation) in seconds

a,*b* : coefficients (which depend on recording system and site condition)

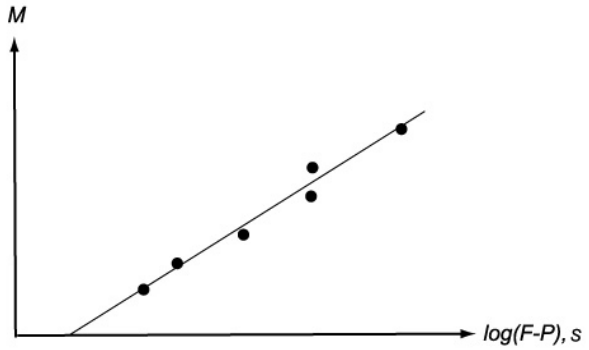

Fig. 6.2 *F-P* times against magnitudes.

Tsumura (1967) assumed the following equation:

$$M = a\log(F-P) + b + cD$$

where D is the epicentral distance in km. He applied this formula to data at the Wakayama Microearthquake Observatory, Earthquake Research Institute, University of Tokyo, Japan, and obtained the following formulas:

$$M = 2.85\log(F-P) - 2.53 + 0.0014D$$
$$M = 2.85\log(F-P) - 2.36 \quad (D<200 \text{ km}) \qquad (6.1)$$

Lee et al. (1972) also established the same empirical formula for estimating magnitudes of local earthquakes recorded by the USGS Central California Microearthquake Network using signal durations. Their formula is

$$M = 2.00\log(F-P) - 0.87 + 0.0035D. \qquad (6.2)$$

After these studies, the *F-P* magnitude became widely used in microearthquake observation, as in the following two examples.

$$M = 2.97\log(F-P) - 2.56 \quad \text{in SW Honshu (Oike, 1975)} \qquad (6.3)$$
$$M = 3.65\log(F-P) - 4.26 \quad \text{in the Philippines (Uy, 1985)} \qquad (6.4)$$

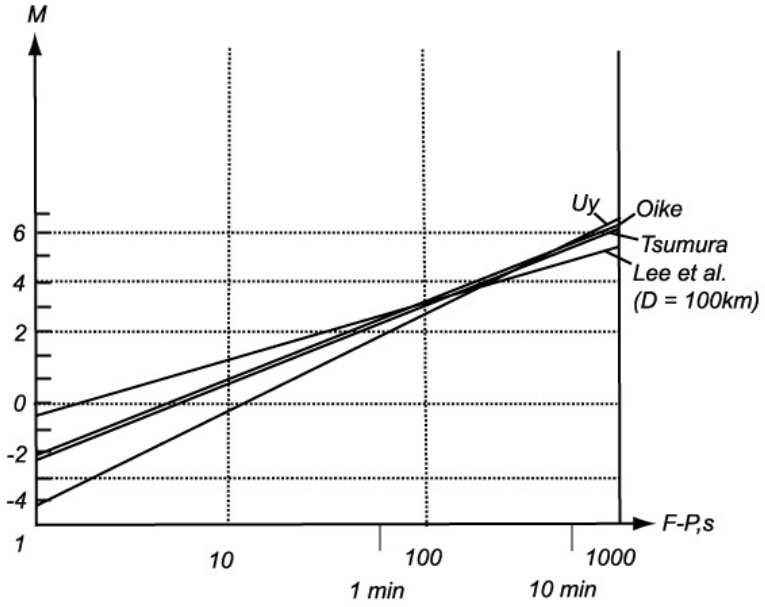

Fig. 6.3 Comparison of formulas (6.1) - (6.4).

All formulas above are plotted in Fig. 6.3. Although coefficients differ, their estimated *F-P* magnitudes are almost identical at $M = 4$, because when they made their formulas, much data whose magnitudes is about 4.

This magnitude scale has the following advantages:

1. Coverage of a wide range of magnitude with a single seismograph, without problems such as saturation or underexposure in the case of maximum amplitudes.
2. Simplicity of treatment, especially for the earthquakes with short epicentral distances.
3. Applicability to earthquakes whose hypocenters are unknown.

It has the following shortcoming, however:
If a second event occur, before a first event finishes, it is not possible to measure the total duration time of the first event.

Theoretical and empirical background of the formula is as follows: *S* coda waves are backscattered *S* waves of the incident direct *S* wave due to heterogeneous media. The coda duration time is therefore nearly constant regardless of its epicentral distance or azimuth (cf. Yomogida, 1993).

Exercise 6.2 Calculate the *F-P* magnitude of the event shown in Fig. 6.1 using equation (6.3).

Exercise 6.3 Obtain the *F-P* magnitude formula for local earthquakes as follows: Suppose we are

carrying out earthquake observation in Japan and observed 5 larger events of which magnitudes were determined by another permanent seismic network, such as the JMA. Listed are the observed *F-P* times and standard magnitudes determined by the JMA. Note that semi-logarithmic graph paper instead of section paper is used:

Table 6.1 Observed *F-P* times.

Event No.	*F-P*, s	M_{JMA}
1	100	3.1
2	410	4.8
3	215	4.0
4	83	2.7
5	238	4.3

Exercise 6.4 Observe the magnitude 1 and 6 local earthquakes on the Wakayama network, Japan. What are expected total duration times of 2 events?

Exercise 6.5 If we observe events by an event-triggered system, we cannot record whole waves. Is it possible to obtain a formula?

6.3 Magnitude Scales Used by ISC and NEIS

Ms and *Mb* are used by the International Seismological Centre (ISC) and the National Earthquake Information Service (NEIS) of US Geological Survey (USGS).

Ms: Surface-wave magnitude

$$Ms = \log\frac{A}{T} + 1.66\log\Delta + 3.3$$

where A, T, and Δ are the horizontal or vertical amplitude of surface wave in microns, its period in seconds, and the epicentral distance in degrees, respectively. T is about 20 seconds.

Mb: Body-wave magnitude

This is calculated by the same formula as *mB* below.

mB: Body-wave magnitude by Gutenberg

$$mB = \log\frac{A}{T} + q(\Delta, h)$$

Correction term $q(\Delta,h)$ is a function of Δ and h, and its range is about from 6 to 8. T is several to ten seconds.

References

Lee, W. H. K., Bennett, R. E., and Meagher, K. L., 1972, A method of estimating magnitude of local earthquakes from signal duration, Geol. Surv. Open-File Rep.(U.S.), 28.

Oike, K., 1975, On a list of hypocenters compiled by the Tottori microearthquake observatory, Zisin (J. Seism. Soc. Japan) Ser. 2, 28, 331-346 (in Japanese with English abstract).

Tsumura, K., 1967, Determination of earthquake magnitude from total duration of oscillation, Bull. Earthq. Res. Inst., Univ. Tokyo, 45, 7-18.

Uy, E. A., 1985, Magnitude determination from time duration of body waves, Bull. Intern. Inst. Seism. Earthq. Engineer., 21, 87-92.

Watanabe, H., 1971, Determination of earthquake magnitude at regional distance in and near Japan, Zisin (J. Seism. Soc. Japan) Ser. 2, 24, 189-200 (in Japanese with English abstract).

Yomogida, K., 1993, Surface waves and scattering and attenuation of seismic waves, IISEE Lecture Notes.